Simulation of an Artificial Respiratory System

2010

A. Delawari & R. Doelman

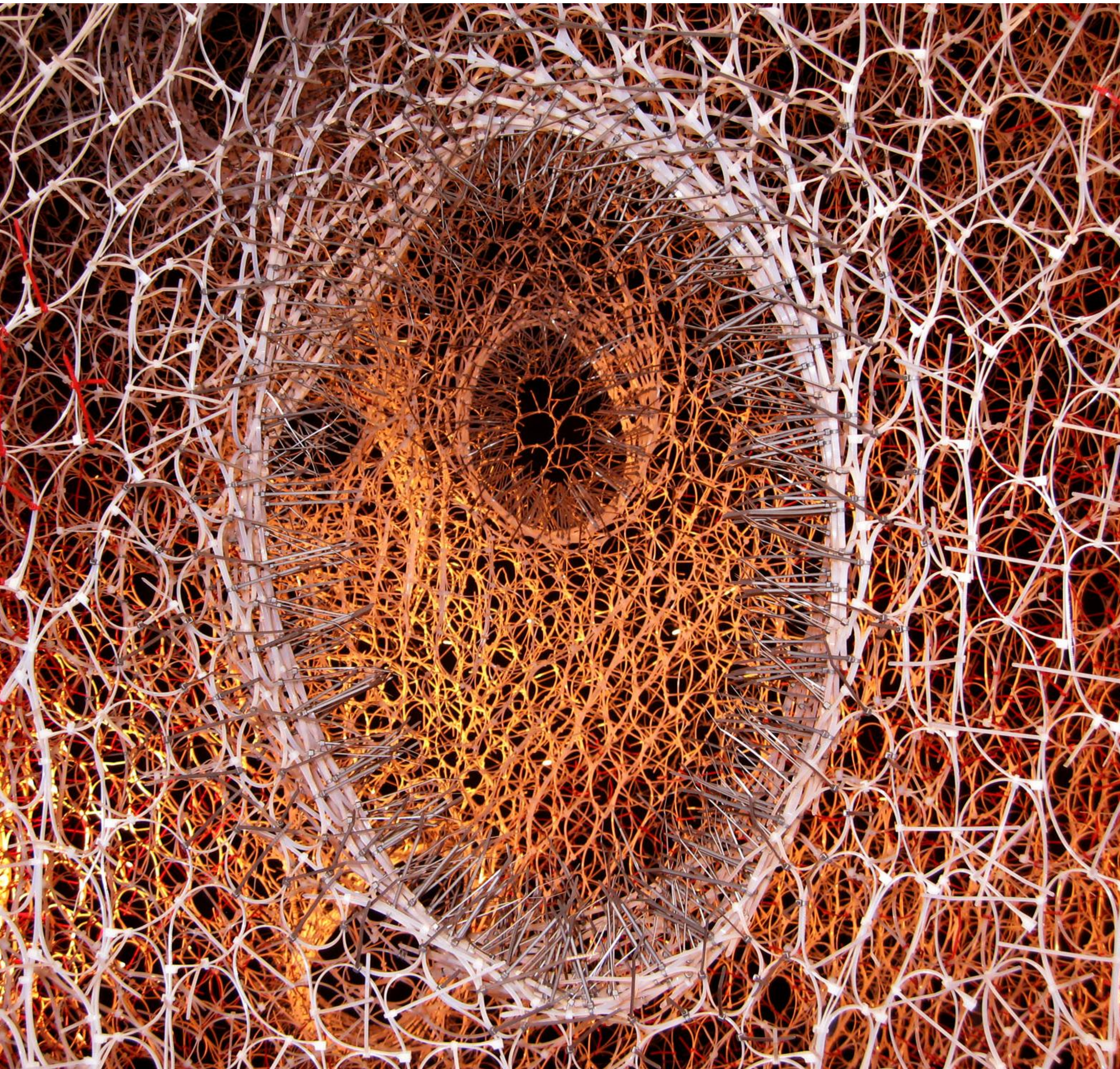

Simulation of an Artificial Respiratory System

Choosing a New Actuator for Implementation in a Lung Simulator.

Anton Delawari

1362518

Reinier Doelman

1354639

Coordinator:

Prof. Dr. R. Babuska

Delft University of Technology

Delft, 2010

Cover: ***"Branching Morphogenesis"***

by Jenny Sabin, Andrew Lucia, Peter Lloyd Jones and Annette Fierro.

An installation of tie-wraps, where each tie-wrap represents a force exerted by lung cells on proteins surrounding them as they form lung capillaries

Table of Contents

Preface

In this thesis we present an analysis of different actuators for the use in a lung simulator. We chose this subject, because the idea of contributing to a better healthcare is very satisfying. In the process, we learned that engineering is much more than completing textbook exercises. For one, we were the ones that set our own 'exercises'. Also, many times there was more than one answer, and not necessarily was there an incorrect answer. We learned that the most important thing is that you have to choose what you will continue with on the way to the eventual goal of the project.

We like to acknowledge all the help we had from all those people, whom without this thesis wouldn't have been the way it is now.

We'd like to thank:

- Prof. Babuska for guiding us from start to finish.
- The people from IngMar Medical, for being so kind to lend us one of their lung simulators, and also the technical staff from the faculty 3ME for preparing an experimental setup.
- Maureen Mekel, for asking the right questions to find a way out when we were stuck on the project.
- Ton Verbraak for taking the time to answer our questions on the ethical aspects of engineering.
- Dr. Henk Stam, Wim Holland and Ton Verbraak from the Erasmus Medical Centre for telling us what the medical and technical requirements of a lung simulator are.
- Dr.ir. H. Polinder for telling us about different electromechanical actuators.
- Dr.ir. A. van der Weiden for showing us some possibilities for the control system.

Finally, we'd like to thank Drs. W.J. Blokzijl for proofreading our thesis

Reinier Doelman & Anton Delawari

Delft, 2010

Summary

The current generation of lung simulators by IngMar Medical doesn't fulfil all the requirements imposed by its users, scientists and doctors. This research is conducted to look for possible actuators to replace the brushless dc motor, which is now used and is the bottleneck for further development in the area of ventilation equipment, because this actuator cannot be used to simulate certain lung pathologies. This report represents the research done and explains the choices that are made along with their considerations.

Delays in feedback loop cause instability

The brushless dc motor is not backdrivable. This is compensated for by a feedback loop to simulate ventilated breathing. This feedback loop causes inherent delays, allowing for overcompensation and causing instability in the system.

A voice coil actuator is the most suitable option

After considering different types of actuators, two types seem most suitable: the voice coil or the permanent magnet linear synchronous motor. After analyzing both of them and comparing these to the preferences and requirements for the actuator, the voice coil is chosen as the best candidate to prove that backdrivability can solve the instability problems.

With voice coil actuators there is a trade-off between force and stroke. This problem is to be further investigated in future research. For implementation, possible solutions could be a configuration of actuators, further development of this actuators or a mechanical solution to get to required force and stroke, though backdrivability could be affected for the worse in all of these solution.

A novel system design using a voice coil can solve the instability problems

It is shown in simulations that a different setup for the system than the setup for the brushless dc motor, using a voice coil, can simulate more lung pathologies than the old setup can. Input voltages for the voice coil are realistic and the accuracy depends on what input voltage the voice coil can take on.

Extensive tests not carried out due to lack of time

A test with the IngMar Medical ASL5000 wasn't performed. Test with this and other actuators were out of reach, due to lack of time and technical problems. Possible setups for experiments are discussed in the appendix for further research.

Recommendations for future research

The development of the spiral actuator is very promising. A closer could be given to this design and its applications. It is expected that it would be a more suitable actuator for this application, because of longer stroke with a required amount of power in a more compact device, without any additional mechanical aid.

Also, according to research by Gunawan, Muijs and Veljacic the 'ironless core' actuator would be best suitable for implementation. In future research this actuator could be put to the test.

1 Introduction

The demand for simulation devices of the human body is rising, because many enterprises, universities and organizations are active on the medical market with both profit and non-profit goals. For them it would speed up the process of designing, prototyping and testing new, advanced lung ventilators if they can test their designs on accurate simulators and not on patients, who are not always at hand, not always prepared to cooperate and who would suffer greatly if anything goes wrong in the process. If we could just develop a simulator that simulates the human lungs, rapid innovation would be beneficial to many patients that suffer from a whole range of different lung illnesses.

The problem with the best available lung simulators these days is that their inner workings are not suitable to simulate all different lung pathologies and illnesses. The actuator that simulates the breathing motion doesn't accurately respond in certain situations. To overcome this problem a different type of linear actuator needs to be chosen. The hypothesis is that the cause of these problems is that the current actuator doesn't respond (enough) to load disturbances.

Can a backdrivable actuator solve the instability problems of the current generation of lung simulators?

In this report several different actuators are analyzed that according to recent pre-research by [1] promise to be good replacements.
To answer this question the following methods are used:

- Interviews with medical and technical specialists
- Literature
- Mathematical modelling
- Computer simulations

For this research several preconditions are posed by the medical environment the simulator is used in and the need to improve over the current generation of lung simulators.

The structure of the report is as follows. In the first chapter a closer look is taken at the human lungs and what characteristics of these lungs are important. The current generation of lung simulators is analyzed in chapter 3. The issues that arise are translated into requirements in chapter 4. In the fifth chapter different alternative actuators for the next generation of lung simulators and their mathematical models are discussed. The most promising actuator is simulated in chapter 6 in two different setups and the results are analyzed.

2 The respiratory system

Lung simulators are supposed to have similar behaviour to normal human lungs. To design such a device, an understanding of the structure and working of the lungs is necessary. This chapter covers the lungs and how they work. In the first section relevant information of the lungs' workings are described and the section is concluded with the requirements for the device. The mathematical model and simulation are discussed in section 3 and 4 respectively.

2.1 Lungs

The metabolic reaction of glucose with oxygen ('aerobic respiration') delivers 18 times more energy than without it ('anaerobic respiration') in the so-called 'Citric Acid cycle' or Krebs cycle [**2**]. It is clear that the constant inflow of oxygen and outflow of carbon dioxide is critical for the human body.

The air around us consists of 21% oxygen and 0.03% carbon dioxide while the exhaled air has 17% oxygen and 3-4% carbon dioxide [**3**]. The question arises: how do people breathe?

When breathing in, the air flows through the nose and the nasal cavity to the larynx. Past the larynx it flows through the trachea to the primary bronchi. These bronchi are split in secondary bronchi and secondary in tertiary and so on.
The number of branches along a path (sometimes called generation number) is 23-27 [**4**]. The last generation of tubes end in bunches of tiny round air sacs called 'alveoli'. In the alveoli the exchange of oxygen and carbon dioxide from the air with the gasses in the blood takes place (Figure 2.1).

2.2 Properties of the lungs relevant to this project

During inhalation, the diaphragm and the muscles between the ribs contract to increase the space inside the chest and the lungs expand. As they expand, air is sucked in through the nose or mouth because of the pressure difference in and outside the lungs. When a breath is released, the diaphragm and rib muscles relax to make the size of the chest cavity smaller. As this happens, air, rich in carbon dioxide, is forced out of the lungs and airways, and then out of the nose or mouth. (Figure 2.1) [**5**]

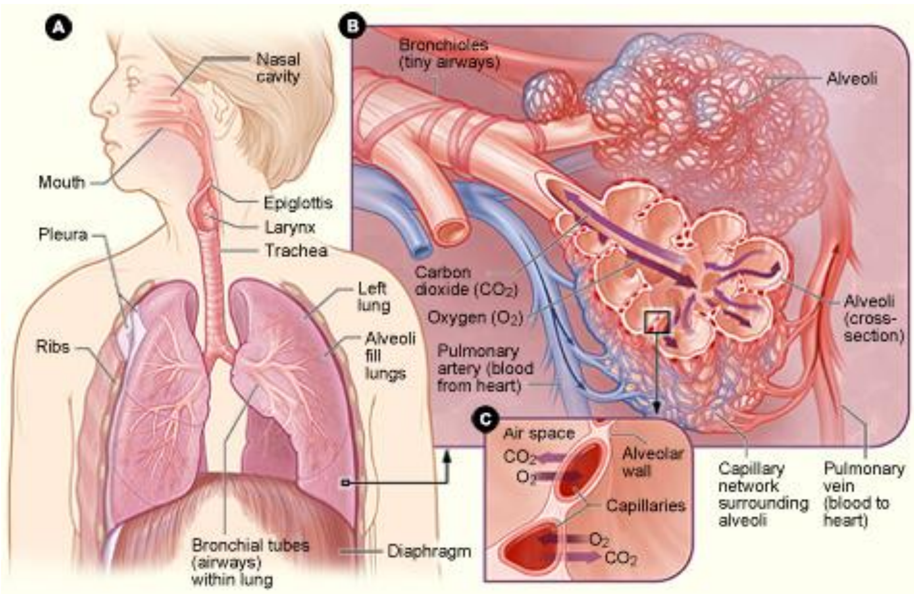

Figure 2.1 – (a) Location of the respiratory structures in the body. (b) Enlarged image of airways, alveoli, and the capillaries. (c) Location of gas exchange between the capillaries and alveoli. [5]

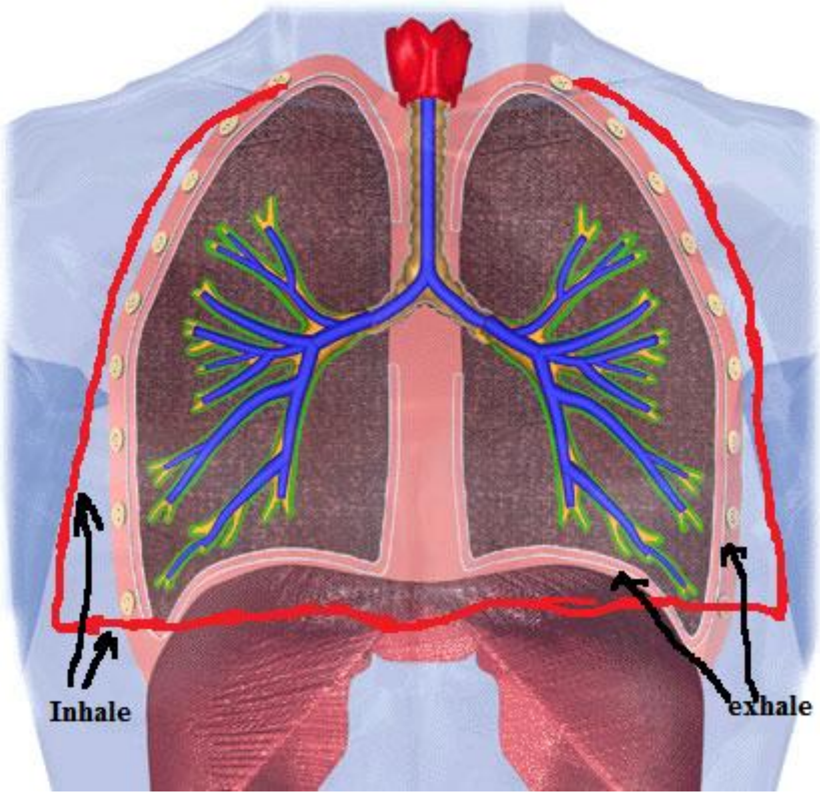

Figure 2.2 - Illustration of human body changes by breathing. [5]. Edited by authors.

2.2.1 Static characteristics of lungs

During normal breathing 500ml of air flows through the lungs (TV in Figure 2.3). Inspiratory Reserve Volume (IRV) is the volume of air that after normal inhalation can be breathed in (2.5 liters). Expiratory Reserve Volume (ERV) is the volume of air that can be breathed out after normal exhalation (1.5 liter). Residue Volume (RV) is the volume of the air that stays in the lungs after maximal exhalation (1.5 liters). Thus, the total capacity of the lungs is

$$TC = (IRV + V_T + ERV + RV) = 6 \; liter$$

The Vital Capacity (VC) of the lungs is the volume of the air that after maximal inhalation can be maximal exhaled.

$$VC = IRV + V_T + ERV = 4.5 \; liter$$

Functional residue capacity (FRC) is the volume of the air after normal exhalation, still presents in the lungs.

2.2.2 Dynamic characteristics of lungs

There are two main characteristics. The most important characteristic of the dynamic behaviour of lungs is the volume of air that can be exhaled after maximal inhalation within one second. In normal circumstances this 'one second' value is about 83% of the VC (Figure 2.3). The next parameter of the lungs is the breathing frequency which for the average person is 15 times per minute (1/4 Hz).

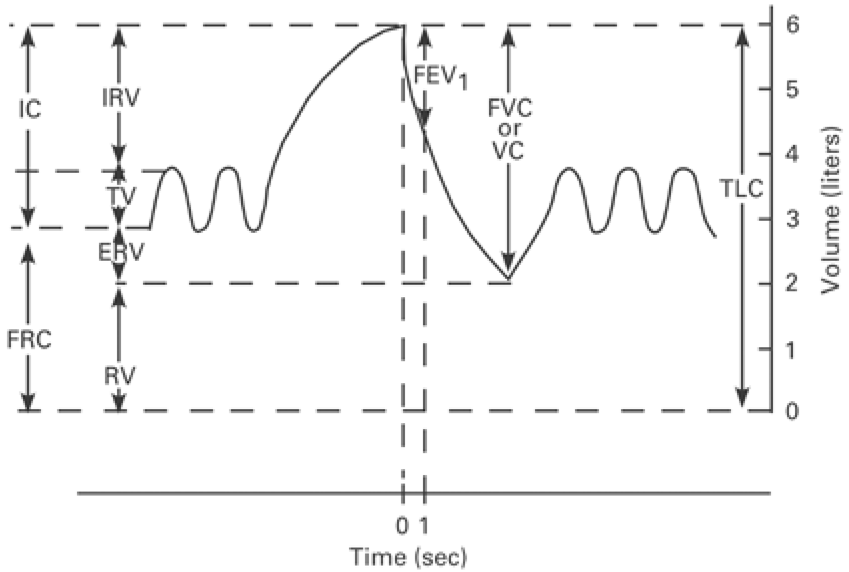

Figure 2.3 - Static and dynamic characteristics. [6]

All the values mentioned before are valid for the average person. From a technical point of view the peak values are more important. To find the peak values, doctors and technical staff[1] of the Erasmus Medical Center were interviewed. As a result the peak values are listed below:

- TC = 8-10 litres,
- 'One second' value = 8.3 litre/sec

The described lung parameters lead to the requirements that the simulator has to fulfil.

2.2.3 Requirements

The most important properties of the lungs are, first, the speed of in- and exhaling, and second, maximal volume. The air compartment of the lung simulator must be larger than 8 litres to be able to simulate patients with a large lung volume. As to speed, it has to be fast enough to suck and push out 20 litres a second within a tenth of second, demanding an acceleration 200 L/s^2 .

Up till here it hasn't been mentioned that lungs are backdrivable, viz. if they are being actively ventilated, they have to follow the breathing pattern of the ventilating device.

2.3 Model

There are a lot of mathematical models of the respiratory system. However, none of these can describe all behaviour of the lungs, because of its irregularities and non-linearity. A lot of models are a good approximation of reality, for example models discussed in work of De Jongh [6] or M. Rozanek and K. Roubik [7]. These are very advanced models, but that is not required for this project. The simpler models discussed in [8] and [9] are more suitable for this project, because the complexities of human lungs fall outside the scope of this project.

[1] Dr. Henk Stam, W. Holland and A. Verbraak (author of [32], co-author of [9]). The minutes of this interview are appended in appendix A.

For this project the following mathematical model of lungs and air compartment is used [10]:

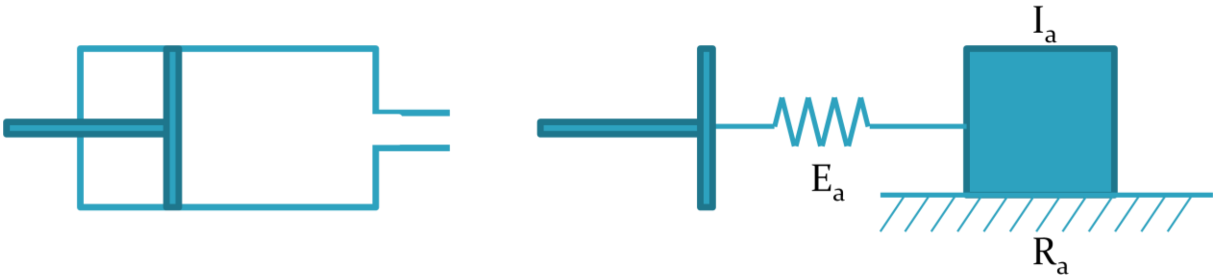

Figure 2.4 - Air compartment (left) and mechanical analogue (right).

The lung characteristics that describe the dynamics of lungs due to external (mouth) pressure are given by [7] as:

$$I_L \frac{d^2V_L(t)}{dt^2} + R_L \frac{dV_L}{dt} + \frac{1}{C_L} V_L(t) = p_m(t) \qquad (1.\ 1)$$

Where R_L, C_L, I_L are the resistance, compliance and inertance of the respiratory system, respectively, V_L the lung volume and p_m the lung volume.

The lung resistance is the force that opposes air flowing into the lungs and is caused by, for example, the bronchi en trachea.

The lung compliance models the ability of the lungs to stretch when inhaling, which is caused by the muscles in the chest and diaphragm.

The lung inertance is due to the acceleration of the gasses in the lungs and the acceleration of the muscles in chest, diaphragm etc. [**8**]

These dynamics are to be simulated, and the dynamics of the air compartment are to be used simulating these.

The air compartment has a pressure-volume dynamic that is given by [7] as:

$$I_a \frac{d^2V_o(t)}{dt^2} + R_a \frac{dV_o(t)}{dt} = E_a(V(t) - V_o(t)) = -p(t)$$

Where I_a, R_a, E_a, V and V_o are the air inertance, tube flow resistance, air compressibility, current volume of the compartment, and the volume of the outgoing air, respectively and p is the internal pressure of the compartment. It is a linearized model of the internal effects in the compartment.

The model has to follow pressure and flow through the mouth as depicted in Figure 2.5, but for analyzing signals, we use a square-wave pulse for a ventilator.

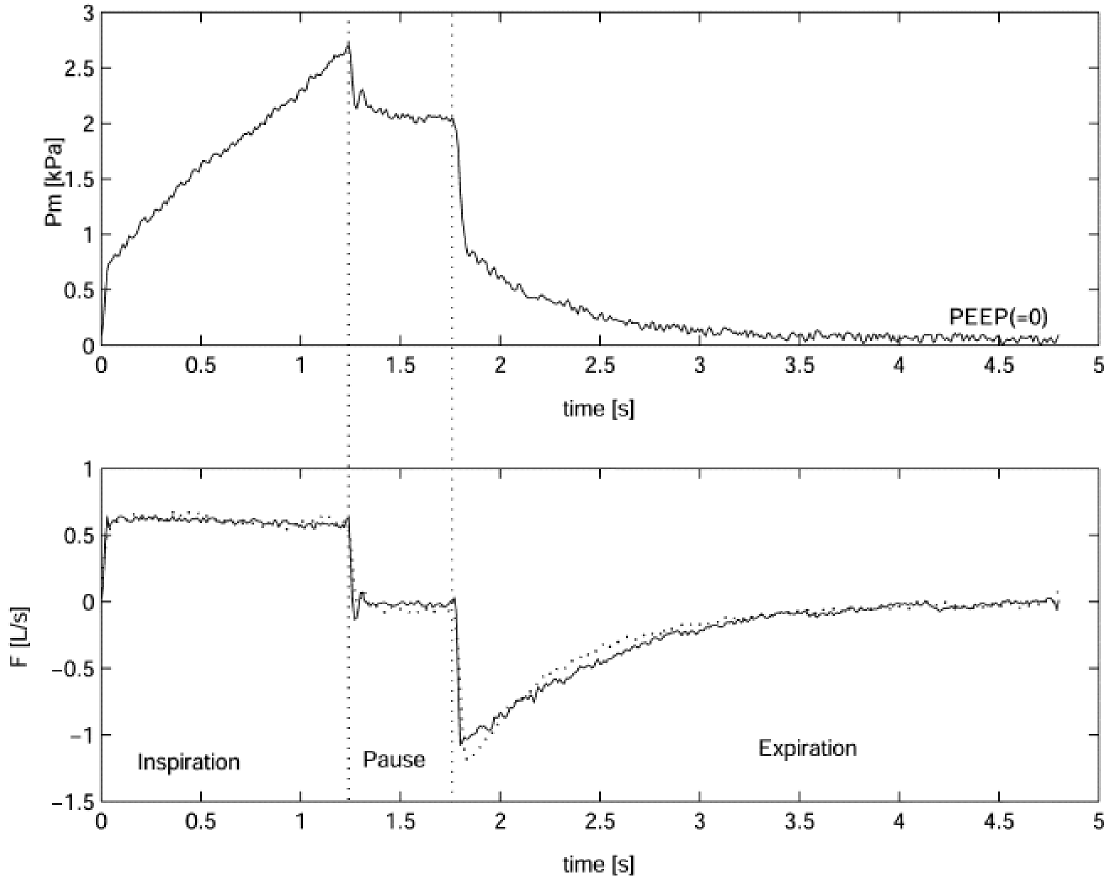

Figure 2.5 – Pressure and flow through mouth. [9]

2.4 MATLAB simulation results

The system depicted in Figure 2.6 is simulated in MATLAB. The 'Lung Model' block has a transfer function:

$$\frac{V(s)}{p_m(s)} = \frac{C_L}{R_L C_L s + 1} \qquad (1.2)$$

Where $V(s)$ is the lung volume, $p_m(s)$ is the mouth pressure, C_L is the lung compliance and $R_L$is the airways resistance. This is derived from equation 1.1 by setting I_L to zero.

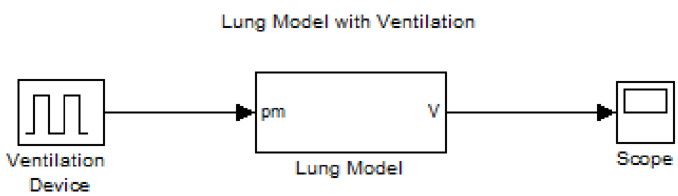

Figure 2.6 - Ideal situation lung model

The result is depicted in Figure 2.7.

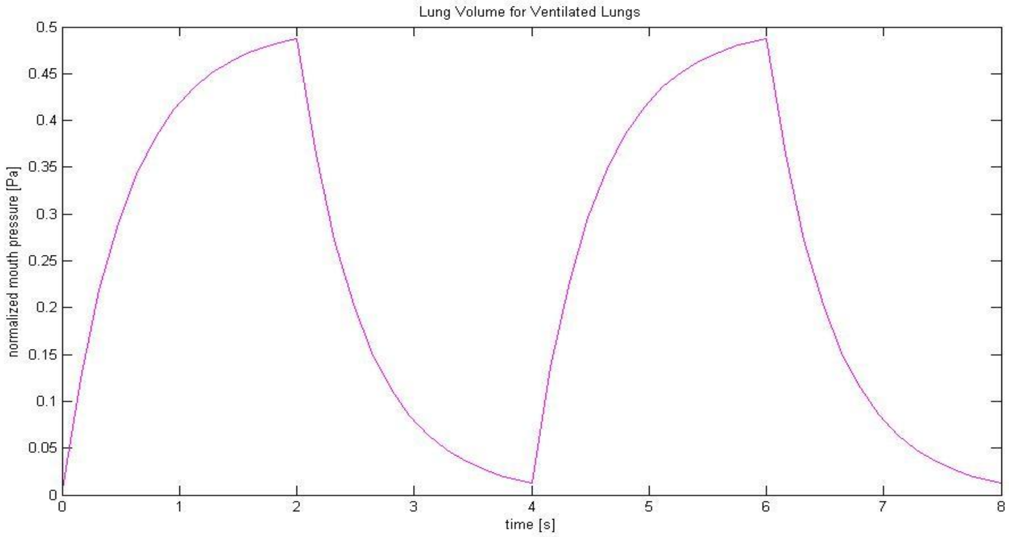

Figure 2.7 – Lung volume for ventilated lungs

On the vertical axis the normalized mouth pressure is depicted, in Figure 2.6 this is the input for the block 'Lung Model Ideal'. The ventilator frequency is one cycle every 4 seconds.

This doesn't resemble Figure 2.5, because the lung is ventilated with a different pressure signal, a square wave instead of the pressure depicted in Figure 2.5. There are some similarities: when the pressure drops and the lung exhales, an exponential decrease is visible, seen as an exponential increase in (negative) flow.

3 The IngMar Medical ASL5000 lung simulator

In this chapter the problems with the most advanced lung simulator available on the market, the ASL5000 are discussed. In the first part of the chapter ASL 5000 from IngMar Medical is discussed and especially the main throwback of its design. In part two the brushless DC motor, the actuator used in the ASL5000 is discussed with corresponding mathematical model. The chapter is concluded with simulation of the system, where the problems in the design of the ASL5000 are shown.

3.1 Analysis of the IngMar Medical ASL5000

There are not many lungs simulators due to limited demand. Most of them are not professional solutions and don't fulfil the wishes of users.

The ASL5000 from IngMar Medical[2] is the most advanced lung simulator that exists. It can simulate spontaneous and ventilated breathing. The simulator consists of an air compartment, piston, actuator and control unit. The piston that is driven by the actuator makes a linear movement inside the air compartment; this simulates lungs inhaling and exhaling. The screw connected to the piston is screwed in and out the air compartment by a servo motor.

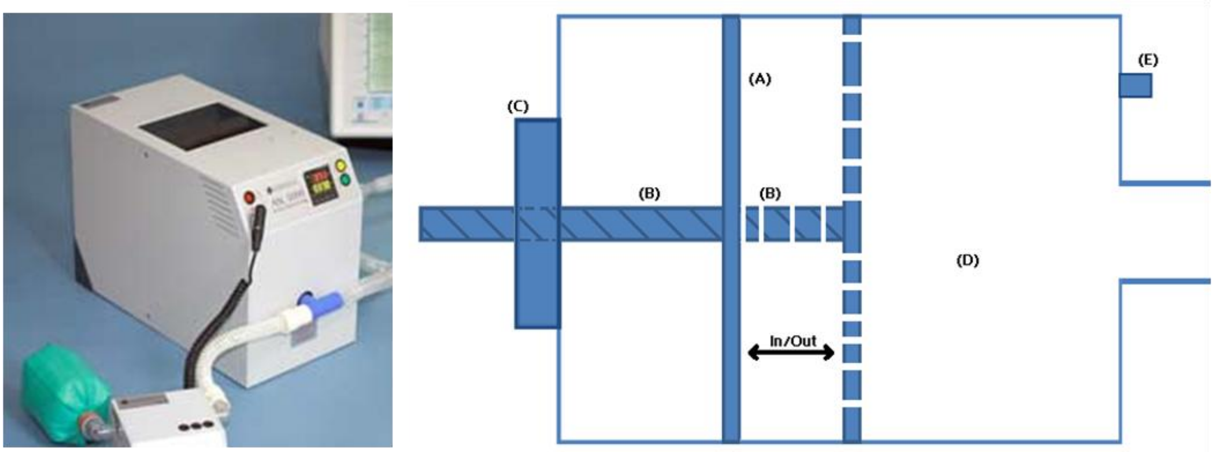

Figure 3.1 - A picture of the ASL5000 (left) and a schematic drawing (right) of the compartment with (a) the piston, (b) the screw, (c) the servo motor, (d) the air compartment and (e) the pressure sensor.

The most important features from a technical point of view for this product are listed below.

Property	Value
Total volume	3.1 L
Tidal volumes	2 to 2700 cm^3 "FRC" setting adjustable (200 – 1500 cm^3)
Spontaneous	Breath rate 0 to 150 per minute
Peak flow	180 L per minute ± 10% (t_{90} Flow < 50 ms)

The total volume of the air compartment is much smaller than the volume of human lungs (see paragraph 2.1). The volume of this air compartment is hardly enough to simulate maximal inhalation of the average person. It's not possible to simulate maximum inhalation followed by maximum exhalation with the ASL5000.

[2] Ingmar Medical's website: http://www.ingmarmed.com/. [34]

A peak flow of 180L/min or 3 L/sec is also exceptionally small. From the study in chapter 2 it should be at least 8 L/sec for the average person. For the best performance a peak flow up to 15L/sec is required.

All above mentioned parameters are strictly dependent on the choice of the actuator. The actuator is a brushless DC motor (BLDC). It is a servo motor that is used which makes a linear movement of the piston from a rotation by use of a (screw) gear. The throwback of this approach is the translation of the rotational movement to a linear movement: backdrivability becomes barely possible, because of friction in the gears.

In ASL5000 the non-backdrivability of the motor is compensated by a feedback loop. In case of external pressure, a sensor detects the differences between the pressure level and the desired pressure level. This is translated via a feedback loop and control unit to a motion compensating for the change in pressure. This approach has a disadvantage due to delays in the feedback loop and causes instability of the system and oscillating behaviour of the motor for some lung parameters.

To be able to simulate the problem a mathematical model of the system is derived in the next section.

3.2 Brushless Direct Current Motor (BLDC)

3.2.1 Working

Brushless motors are similar to the standard DC motor. With the conventional DC motor the current-carrying conductor moves and the magnet is fixed. [**10**]. In the case of the brushless DC motor the magnet and current conductors are reversed. The current to the stator coils is electronically switched in a sequence round the coils so that there is always force acting on the magnet, causing it to rotate in the same direction.

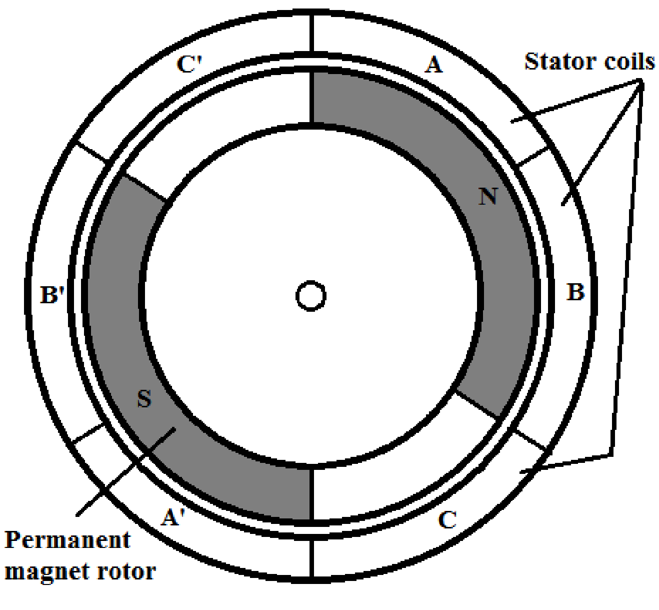

Figure 3.2 - Brushless permanent magnet DC motor [7]

The reasons for the choice of the brushless motor over the brushed are higher torque, speed bandwidths, lower maintenance and robustness [**11**].

3.2.2 Three-phase model

It is assumed that between the input and the motor itself, there is a lossless DC/AC motor. Another assumption is that the 3 phase motor winding, which are symmetrical and identical, are connected in a Y-configuration.

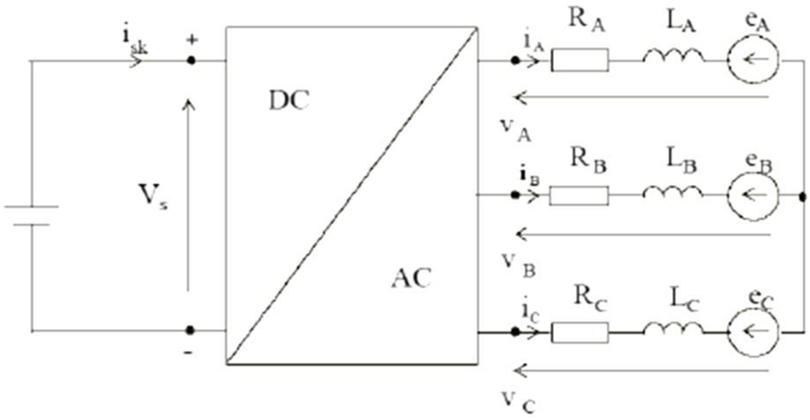

Figure 3.3 - BLDC motor [12]

Kirchhoff's voltage law gives the following equations for the three phase stator winding circuit:

$$v_a = R_a i_a + L_a \frac{di_a}{dt} + M_{ab} \frac{di_b}{dt} + M_{ac} \frac{di_c}{dt} + e_a$$

$$v_b = R_b i_b + L_b \frac{di_b}{dt} + M_{ba} \frac{di_a}{dt} + M_{bc} \frac{di_c}{dt} + e_b$$

$$v_c = R_c i_c + L_c \frac{di_c}{dt} + M_{ca} \frac{di_a}{dt} + M_{cb} \frac{di_b}{dt} + e_c$$

Where $e = K_e \omega_m$ is the back EMF and K_e is the motor torque constant.

It is assumed that $L_a = L_b = L_c = L$, $M_{ab} = M_{ac} = M_{ba} = M_{bc} = M_{ca} = M_{cb} = M$, $R_a = R_b = R_c = R$

Rearranging these equations yields:

$$\begin{bmatrix} L & M & M \\ M & L & M \\ M & M & L \end{bmatrix} \frac{d}{dt} \begin{bmatrix} i_a \\ i_b \\ i_c \end{bmatrix} = \begin{bmatrix} v_a \\ v_b \\ v_c \end{bmatrix} - \begin{bmatrix} R & 0 & 0 \\ 0 & R & 0 \\ 0 & 0 & R \end{bmatrix} \begin{bmatrix} i_a \\ i_b \\ i_c \end{bmatrix} - \begin{bmatrix} e_a \\ e_b \\ e_c \end{bmatrix}$$

The electromechanical torque is:

$$T_{em} = J \frac{d^2 x}{dt^2} + b \frac{dx(t)}{dt} + T_d(t)$$

Where J the motor moment of inertia is; x the position/angle and T_d the disturbance torque is.

The electromagnetic torque for this 3-phase BLCD motor is dependent on the current, speed and back-EMF waveforms, thus:

$$T_{em} = \frac{1}{\omega_m}(e_a i_a + e_b i_b + e_c i_c)$$

3.2.3 Single-phase equivalent model

It's assumed that between the input and the motor itself, there is a lossless DC/AC motor.

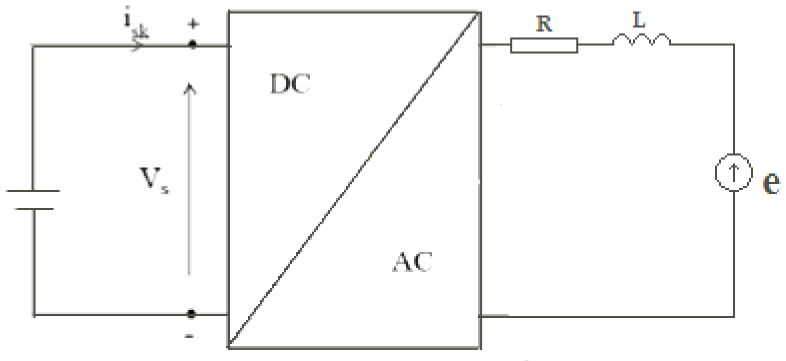

The following equation describes electric circuit:

$$E(t) = Ri(t) + L\frac{di(t)}{dt} + e$$

Where $e = K_e \frac{dx}{dt}$ is the back EMF and K_e is the motor torque constant.

The electromechanical torque is:

$$T_{em} = J\frac{d^2x}{dt^2} + b\frac{dx(t)}{dt} + T_d(t)$$

The electromagnetic torque for this BLCD motor is dependent on the current, speed and back-EMF waveforms, thus:

$$T_{em} = e\frac{i(t)}{\omega_m}$$

Derived above model for the brushless motor is used to simulate the system in the next part of this chapter.

3.2.4 Simulations

To successfully simulate the behaviour of the ASL5000, a MATLAB simulation model is designed after the ASL5000 implementation, as depicted in Figure 3.4

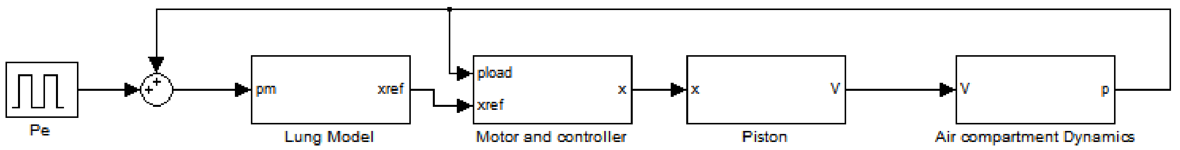

Figure 3.4 - SIMULINK model of a lung simulator using a servo motor.

The lung model is already discussed. To complete the simulation the mathematical models of piston and air compartment has to be derived. A linear mass-spring system is used as an equivalent. See Figure 3.5. The same model as in [7] is used.

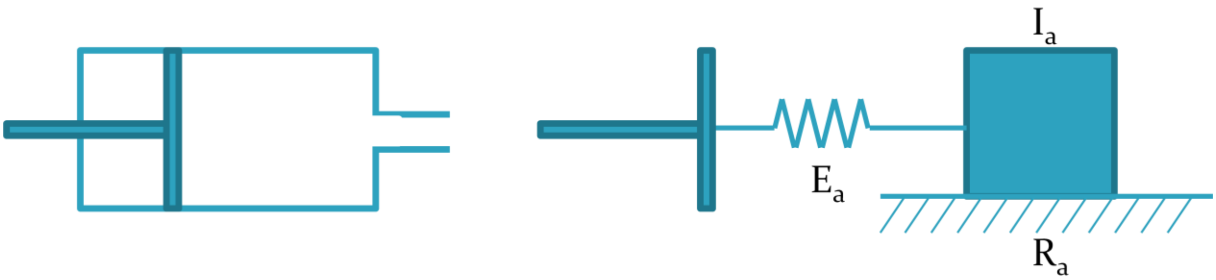

Figure 3.5 - Air compartment (left) and mechanical analogue (right)

Piston

The piston model is a simple gain of the lead screw pitch p_s and A_p, the piston area. The pitch converts the angle of the screw into piston displacement; the piston area converting the piston displacement into volume:

$$V(t) = A_p p_s x(t)$$

Air compartment

The air compartment is non-linear, due to a changing air compressibility modulus with volume. It is assumed, though, that a linear approximation suffices, because the change is small.

From [7]:

$$I_a \frac{d^2V_o(t)}{dt^2} + R_a \frac{dV_o(t)}{dt} = E_a\big(V(t) - V_o(t)\big) = -p(t)$$

Variables

The variables are provided for by IngMar Medical and R. Babuska. The motor is from Bayside Kit Motors, from the frameless motor series. A datasheet is included in Appendix C and the values for the parameters can be found in Appendix E.

Controller

The controller, both for the BLDC and actuators in chapter 5, has two requirements: to a step input, the rise time must be no more than 150 ms, a reasonable time for this motor, and the overshoot has to be 0, to prevent oscillations (in speed and position) and to mimic lungs as close as possible..

3.2.5 Waveforms of the BLDC in a lung simulator

In Figure 3.6, a Bode plot of the actuator is shown. The phase margin (PM) is 83 degrees.

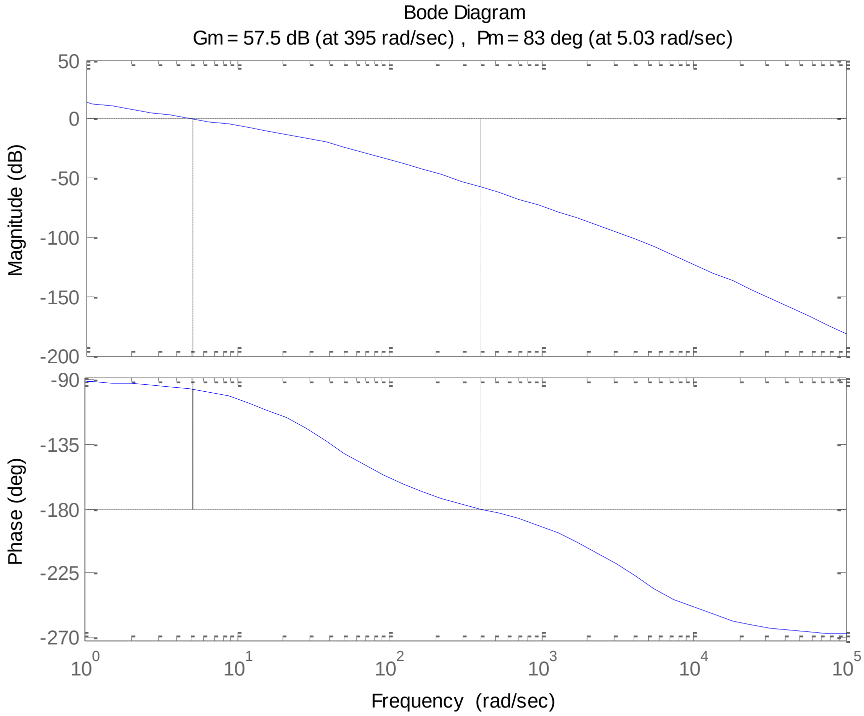

Figure 3.6 - Bode plot for the BLDC motor.

To make a realistic system which is suitable for this application, the following requirements are posed:

- rise time < 0.15 s
- no overshoot
- input voltage < 100V

To make the actuator faster and to add phase to the phase margin, a lead compensator is designed (with help of [**13**]) with the following parameters:

- Gain = 3;
- alpha = 1/10;
- T = 1/30;

The gain is limited due to input voltage requirements.

In Figure 3.7, the Bode plot of the actuator with designed controller is depicted. The gain margin (GM) = 46 dB, and the PM = 93.7 degrees.

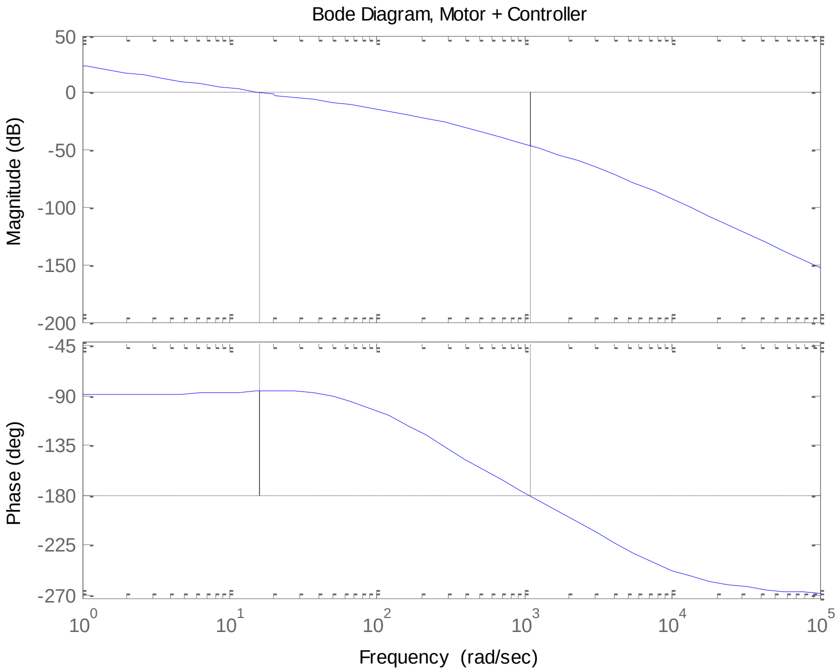

Figure 3.7 - Bode plot of the BLDC with the lead compensator

The open loop system of Figure 3.4 (with the lung model, the actuator model, the piston model and the air compartment model) can be analyzed to see whether the closed loop system is stable. The behavior of the whole system differs for different lung parameters. To check for what lung parameters the system is stable, the system is simulated for lung resistances (RL) from 0.2 to 1.6 kPa/L/s, and for lung compliances (CL) from 0.2 to 1.6 L/kPa. In Figure 3.8 the dependence of the phase margin on RL and CL is plotted.

The volume of normal lungs (CL=0.5L/kPa, RL=1.1 kPa/L/s) is simulated for real lungs, and the

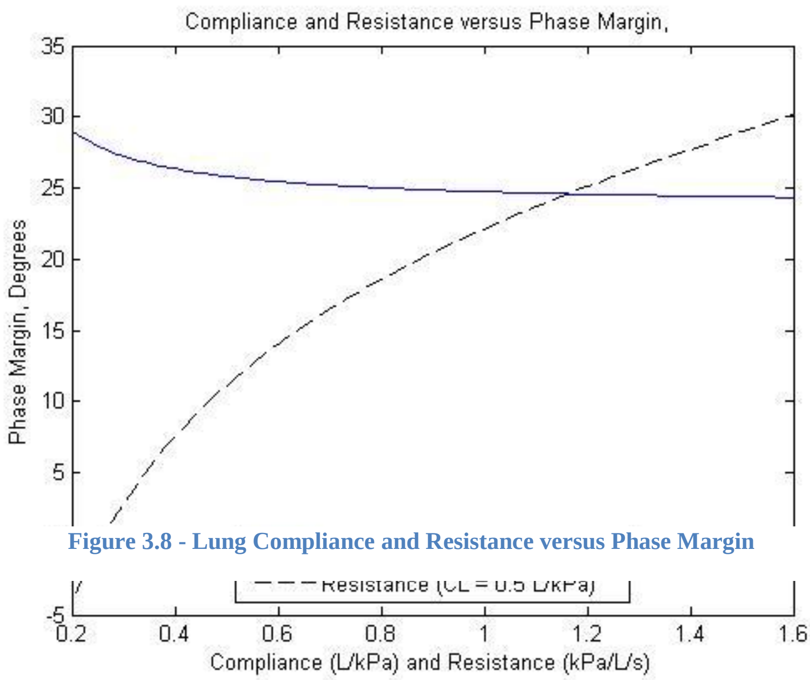

Figure 3.8 - Lung Compliance and Resistance versus Phase Margin

system with an infinitely fast motor and a BLDC with controller (Figure 3.9).

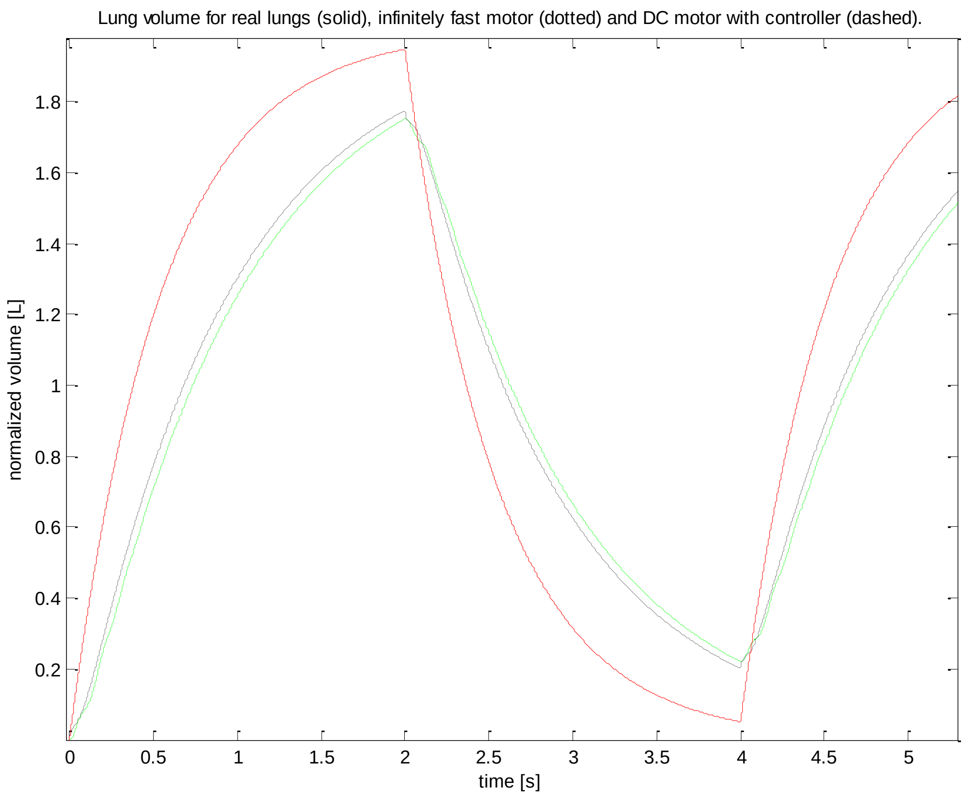

Figure 3.9 - Lung volume for real lungs, a system with an infinitely fast motor and the tuned BLDC

The controller follows the infinitely fast motor, but there is a small difference between the actuator system and the real lung model., but by implementing an extra transfer function, this difference can be compensated for.

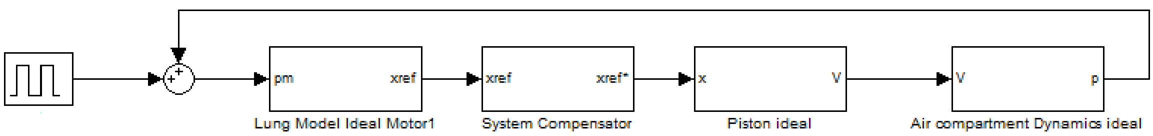

Figure 3.10 - Adjusted system with the System Compensator to compensate for the air compartment dynamics and the closed loop

The transfer function of the the 'System Compensator' block in Figure 3.10 is

$$\frac{1}{1 - L(s)PA(s)}$$

Where $L(s)$ is the transfer function of the lung model, P is the piston gain and $A(s)$ is the transfer function of the air compartment. This compensator ensures the closed loop transfer function of the infinitely fast actuator from p_e to V is exactly $L(s)$ and the BLDC (or any other) actuator follows the path of real lungs. This system compensator could be implemented digitally together with the lung model, which is also digitally implemented.

For extreme low resistance and extreme high compliance the system comes near the instability point.

In Figure 3.11 the simulation of the system with extremely bad parameters are depicted (CL=1.5 L/kPa, RL=0.2 kPa/L/s) which lead to the instability.

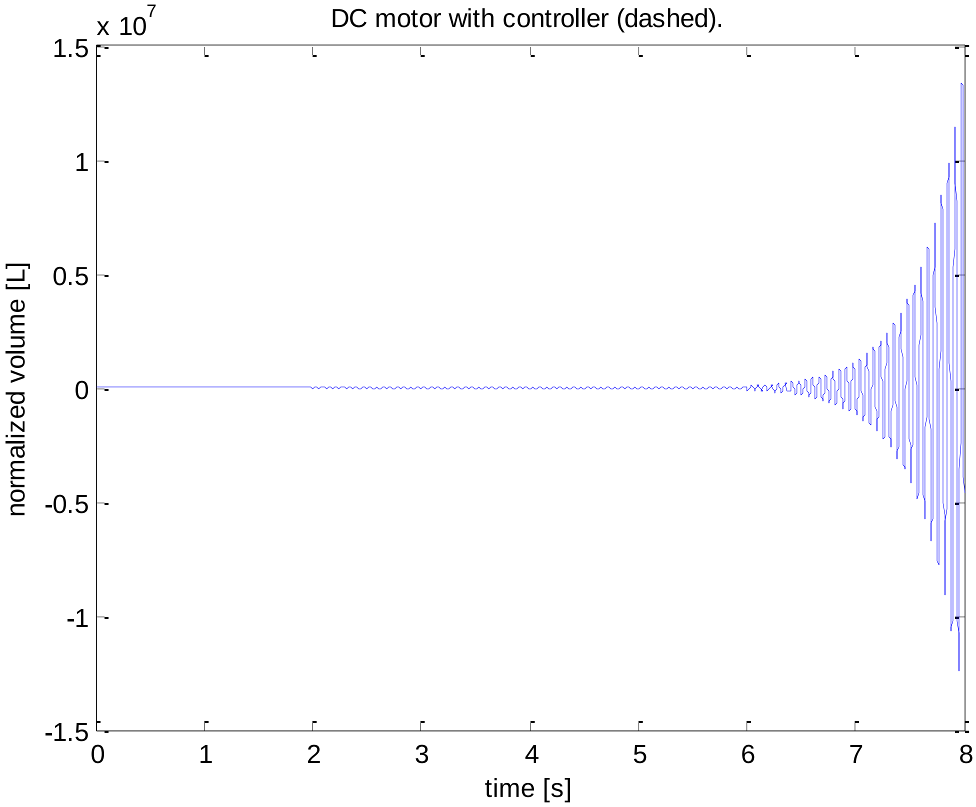

Figure 3.11 - Instable system with very low lung resistance.

3.3 Targets to achieve

What needs to be achieved is clear: design a system that can simulate the lung pathologies that are impossible to simulate with a brushless dc motor and that can cope with these extreme lung parameters.

4 Preferences and Requirements

In chapter 3, it became visible what the limitations to the current generation of lung simulators are. In this chapter, it is formalized as ‘preferences and requirements’ for a new generation of simulators.

4.1 Finding the preferences and requirements

To find these requirements, the flow diagram of Figure 4.1 is used, starting at the top.

4.1.1 Who has the problem?

The main problem stems foremost from technical and medical researchers developing respiratory ventilators. Also doctors specialized in lung diseases, are looking for better devices for calibrating ventilators.

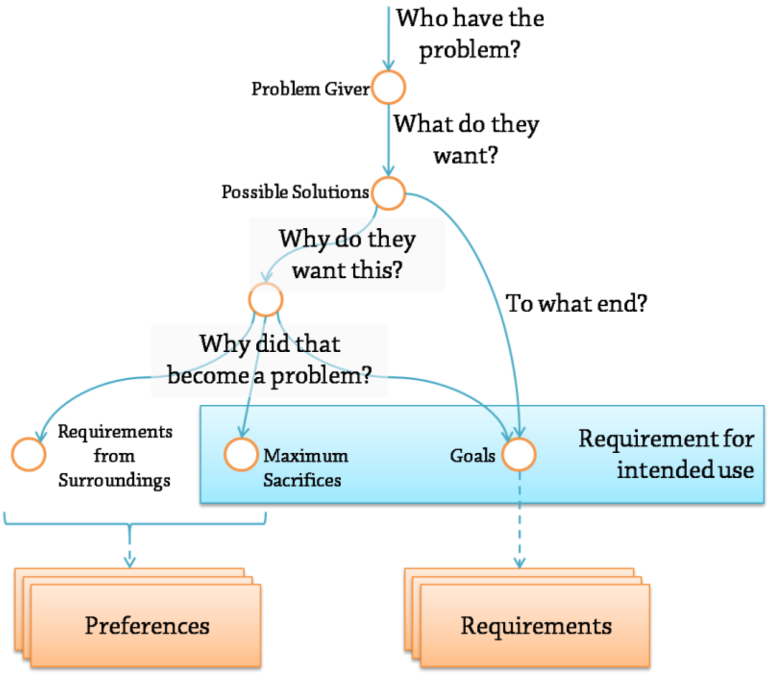

Figure 4.1 - Flow diagram of determining preferences and requirements.

4.1.2 What do they want?

The researchers and doctors are looking for a device on which they can test and calibrate their ventilators as accurate as possible.

4.1.3 Why do they want this?

Researchers want to have a means to test their prototypes on different respiratory illnesses. Patients suffering from these illnesses are not always at hand and a simulator is an easy and safe way to test new ventilators on, without medical procedures.

Doctors, according to an interview[3] with doctor Stam at the Erasmus Medical Centre, Rotterdam, want a calibration device for their lung ventilators to ensure proper behaviour during treatment.

[3] Interview held on May 3rd, 2010. Minutes of the interview in Appendix A

4.1.4 Why did that become a problem?

The previous generation of respiratory simulators couldn't cope with a large enough scope of different lung pathologies, inherent to the choice of driving actuator.

Besides, one could argue it's ethically irresponsible to test new devices on human patients, before proper working is ensured. Testing on patients treats individuals as a means and not primarily as an end in themselves.

Another problem with physical patients is that not all different lung diseases are always at hand and as patients age, their lungs change, so comparing ventilators becomes difficult.

4.1.5 To what end?

The benefits of accurate lung simulators for researchers and doctors are three-ways:

- Testing of prototypes can be done faster, because medical requirements are absent before the final test on patients. This speeds up the design process.
- With the increased scope of lung pathologies, the design can be validated more accurately.
- Doctors can calibrate respiratory equipment.

4.2 Technical Requirements

- The actuator movement is linear (1-DOF).
- The actuator input-output characteristic is linear.
- The actuator is backdrivable.
- The actuator peak force is at least 350N. [**1**]
- The simulator is configurable via MATLAB and LabView.
- The volume displacement is at least the peak lung volume.
- The peak airflow from the simulator is at least that of any patient.
- The power supply input must be 100-240V, 50-60Hz.

4.3 Use, Maintenance and Management Requirements

- The user interface is easy to use.
- The simulator is easy to clean and disinfect.
- The simulator is easy to move.
- The end product must comply with European (and local) guidelines on medical systems.[4]
- The simulator is easy to connect to ventilator.
- The simulator is easy to connect to external computers and the internet over a secure connection.

---

[4] EU Directive 93/42/EEG on medical devices:
http://eurlex.europa.eu/LexUriServ/LexUriServ.do?uri=CELEX:31993L0042:NL:HTML,
EU Directive 2006/95/EG on low voltage application:
http://eur-lex.europa.eu/LexUriServ/LexUriServ.do?uri=CELEX:32006L0095:NL:HTML,
EU Directive on measuring instruments:
http://eur-lex.europa.eu/LexUriServ/LexUriServ.do?uri=CONSLEG:2004L0022:20091201:en:PDF
CE Directive:
http://www.evd.nl/zoeken/showbouwsteen.asp?bstnum=94512&location=&highlight=CE-markering

4.4 Commercial, Strategic and Financial Requirements

- The quality-price ratio must be larger than competitors'.
- The manual and safety stickers must be available in English, Japanese, French.
- The product must be affordable by hospitals in western countries.

5 Alternative actuators for the use in lung simulators

Given the preferences and requirements in the last chapter and the analysis in chapter 3, it is clear not every actuator is as suitable for this application as the next. There is a broad range of actuators, of which some are obviously not suitable, and others need more research to determine this.

5.1 Unsuitable actuators

Actuators that aren't suitable are:

- Wax motor, powered by heating and cooling of wax, are too slow for this application and not accurate enough.
- Hydraulic actuators suffer from losing fluid, are way more powerful than necessary, are not backdrivable and need too much extra equipment to build into a lung simulator.
- Pneumatic actuators are backdrivable, but highly non-linear and need an air compressor (too large to build into a lung simulator and too loud).
- Ferro fluid actuators, a combination of hydraulic and electromagnetic actuators, are too small for this application, and existing designs are non-linear. This is usually used in micro-actuators.[**14**], [**15**]

Some actuators need closer analysis and are almost all electromagnetic actuators, because most of these actuators are very easily backdrivable. They, along with others are researched in [**1**]. Some of the most promising are:

- Voice coil actuator
- Spiral motor
- Piezoelectric actuator
- Linear motor

From these the voice coil, spiral motor and linear motor will be analyzed more closely below.

5.2 Voice coil actuator

5.2.1 Topologies

Several different types of coil actuators exist. The difference between them is whether the coil is moving, 'moving coil', or the iron rod inside the coil, 'moving iron'. The difference is not what is defined as static and what as moving; the designs themselves differ. Other terminologies for 'moving coil' are 'voice coil' or 'Lorentz actuator' (because it uses the Lorentz force), and a 'moving iron' actuator is sometimes called an electromagnet. [**16**]

Moving Iron

Moving Iron actuators are popular actuators that use the force of magnetic attraction. The reason why they are used often, is that these actuators can exert a much greater force than an (in weight) comparable Moving Coil actuator.

Moving Iron actuators exert a force that is inverse quadratic related to the distance between the magnets:

$$F \propto \frac{F_m^2 A}{r^2}$$

Where F_m is the magneto-motive force of the magnets (assumed they are equal), A the surface area and d the distance between the two magnets.[17]

This is their advantage: when r is small, the exerted force is large. But it is their disadvantage also: the exerted force is not linear with distance (not an LTI system) and hence the Moving Iron is difficult to control.

This type of actuator will not be discussed any further, because integrating this into a system will be difficult.

Moving Coil

Moving Coil actuators use permanent magnets and the current through the coil to create motion of the coil. Its force limitations arise mainly from heating of the coil due to large currents. Because the force is linearly dependant on the current and the (constant) magnetic field, it is excellently controllable.

There are two types of voice coils: lateral moving and rotary moving coils.

Lateral

Lateral voice coil actuators are used in audio speakers; hence the name ‘voice coil’. Several designs exist, depicted in Figure 5.1.

A lateral voice coil is a cylindrical wound coil placed in a radial magnetic field. This magnetic field is created by permanent magnets. These permanent magnets have a radial magnetic field because they are themselves tube-like and are magnetized that way. The permanent magnets are connected to the cylindrical iron core on which the coil is wound.

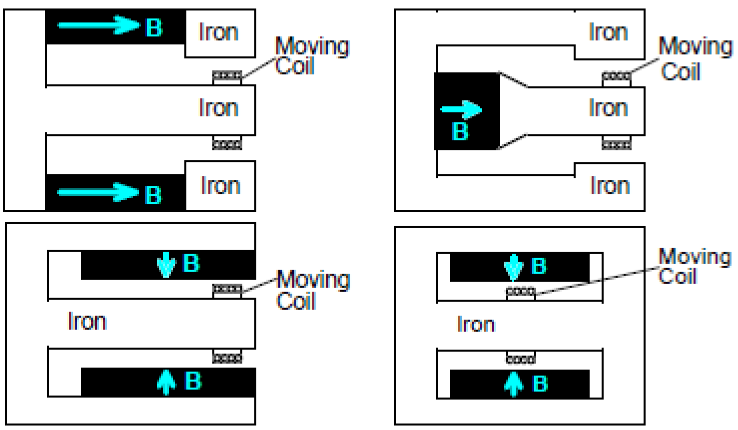

Figure 5.1 - Several lateral voice coil designs. The design in the bottom right corner is sometimes called a ‘slide motor’

Rotary

In Figure 5.2 an actuator of this type is depicted.

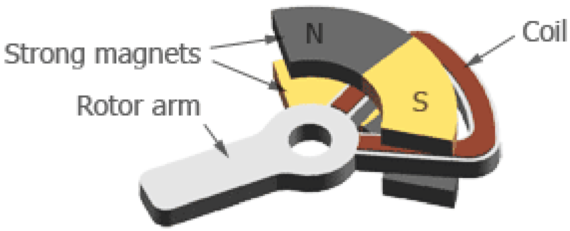

Figure 5.2 - A rotary moving coil actuator. [18]

A rotary voice coil, as can be seen in the figure above, consists of two parts. One is the mover, with on one end the arm and the other the coil. The other is the stator with permanent magnets that create a strong magnetic field. The mover is mounted on a pivot (the ring in Figure 5.2) on which it rotates. When an electrical current flows through the coil, the Lorentz force makes the coil and arm rotate.

Rotary moving coil actuators are often used in magnetic harddisks for the read/write head. In Figure 5.3 a voice coil from a Seagate harddisk is depicted. The coil and the magnet (with the inscription on it) are clearly visible.

Figure 5.3 - A rotary voice coil from a Seagate harddisk. [33]

5.2.2 Mathematical Model

Why a model of a lateral voice coil

To derive a mathematical model of a voice coil a lateral voice coil design, depicted in Figure 5.1 and again in Figure 5.4, is chosen, because the vertical symmetry allows for easy modelling. Here the leakage flux is minimal and can be neglected.

Nomenclature

Symbol	Definition
l_m	Length of the permanent magnet
l_1	Width of the permanent magnet

x	Position of the coil
d	Height of the coil
i	Current flowing through the coil
B_g	Magnetic flux density of the permanent magnets in the air gap
F	Lorentz (Laplace) force acting on the coil
F_{load}	Disturbance force due to the lung pathology
K_f	Electromagnetic force constant
K_g	Electromotive force constant
N_1	Number of turns of the coil
R	Coil and circuit resistance
e	Electromotive force
p	Pressure in the compartment
A	Piston area, cross-sectional area of the compartment

Model

The following mathematical model is derived by with help of [**19**], [**20**] and [**21**]. A more accurate model including temperature effects can be found in [**22**] and an improved design in [**23**] using shorted turns.

In Figure 5.4 the ‘moving coil’ actuator is depicted together with the appropriate variables that are used in the next sections.

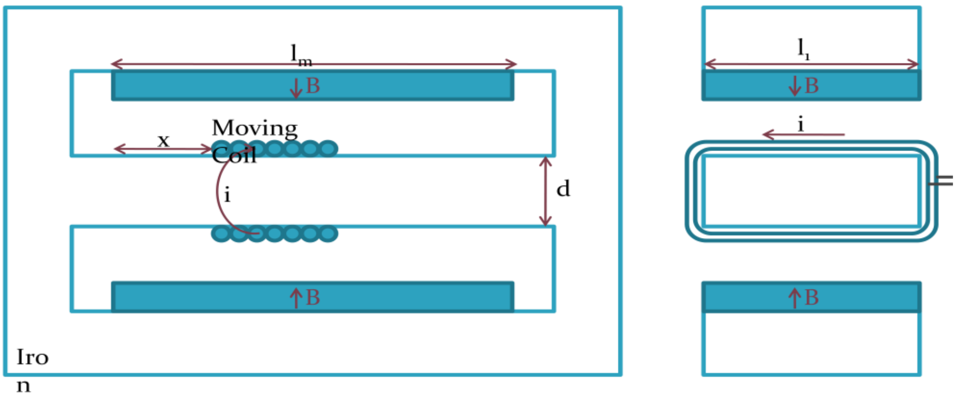

Figure 5.4 - Model of a 'moving coil' voice coil motor and naming conventions.

The electromotive force

The in the coil induced electromotive force is

$$e = \frac{d\psi(t)}{dt}$$

Where ψ is the total flux and $\psi(t) = \psi_1(t) + \psi_m(t)$, $\psi_1(t) = L_1 i(t)$ and ψ_m is due to the flux linkages with the permanent magnet.

$$L_1 = \frac{N^2}{R_{core}}; R_{core} = \frac{l_{av}}{\mu A} = \frac{l_{av}}{\mu_0 \mu_r l_1 d}.$$

The electromotive force due to movement of the coil is

$$e_m(\mathrm{t}) = \frac{d\psi_m(\mathrm{t})}{dt} = \frac{d}{dt}\left(2B_gN_1L_1x(\mathrm{t})\right) = 2B_gN_1l_1v(\mathrm{t}) = K_gv(\mathrm{t})$$

$v(\mathrm{t}) = \frac{dx(\mathrm{t})}{dt}$ and K_g is the electromotive force constant.

Forces acting on the coil

The Lorentz force acts on a charged particle that moves through a magnetic field:

$$\vec{F} = q\,\vec{v} \times \overrightarrow{B_g}$$

Since here there is a straight wire in a right angle to the magnetic field, using the Biot-Savart law, this transforms to the well known formula for the force on a straight wire.

$$\vec{F} = i\vec{L} \times \overrightarrow{B_g} = iLB_g \sin\theta = iLB_g$$

So the force acting on the coil is

$$F(\mathrm{t}) = 2i(\mathrm{t})l_1B_gN_1 = K_fi(\mathrm{t})$$

where K_f is the electromagnetic force constant. Also,

$$K_f = 2l_1B_gN_1 = K_g$$

The electrical equivalent model

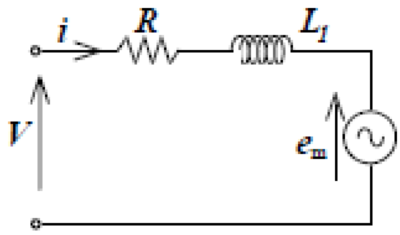

Figure 5.5 - Electrical equivalent model; in the analysis U is used for V, to avoid confusion with the compartment volume

For this equivalent circuit the input voltage U, is

$$U(\mathrm{t}) = Ri(\mathrm{t}) + L_1\frac{di(\mathrm{t})}{dt} + e_m(\mathrm{t})$$

This circuit is a first approximation of a coil. A high frequency equivalent would not be necessary, because the bandwidth of operation is very small and the voice coil operates at low frequencies.

The mechanical equivalent model

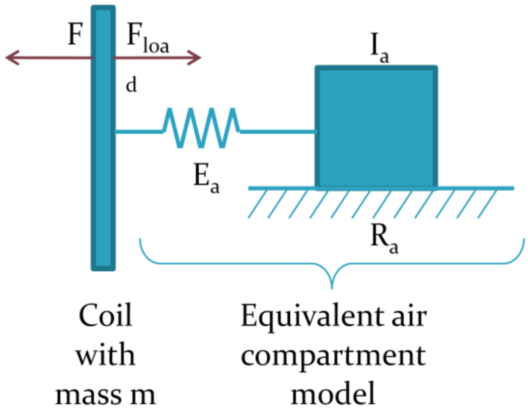

Figure 5.6 - A mechanical representation of the coil with acting force and an equivalent model of the air compartment as load

Newton's second law gives us:

$$m\frac{dv}{dt} = F - F_{load} - bv = K_f i - pA$$

Where p and A are the pressure inside the compartment and the piston area, respectively, and b is the friction coefficient. m is the mass of the coil and the piston.

State equations

Put in time-domain state equations:

$$\frac{di(\mathrm{t})}{dt} = -\frac{R}{L_1}i(\mathrm{t}) + \frac{1}{L_1}U(\mathrm{t}) - \frac{K_g}{L_1}v(\mathrm{t})$$

$$\frac{dv(\mathrm{t})}{dt} = \frac{K_f}{m}i(\mathrm{t}) - \frac{A}{m}p(t) - bv(t)$$

$$\frac{dx(\mathrm{t})}{dt} = v(\mathrm{t})$$

It could be transformed transform this to the Laplace domain:

$$si(s) = -\frac{R}{L_1}i(s) + \frac{1}{L_1}U(s) - \frac{K_g}{L_1}v(s)$$

$$sv(s) = \frac{K_f}{m}i(s) - \frac{A}{m}p(s) - bv(s)$$

$$sx(s) = v(s)$$

Transfer functions

To find the transfer functions from $U(s)$ and $p(s)$ to $x(s)$ superposition is used: first $p(s)$ is set to zero and the transfer function from $U(s)$ to $x(s)$ is calculated; and second, $U(s)$ is set to zero to calculate the transfer function from $p(s)$ to $x(s)$.

$$p(s) = 0$$

$$(L_1 s + R)i(s) = U(s) - K_g v(s)$$

$$i(s) = \left(\frac{m}{K_f}s^2 + \frac{b}{K_f}s\right)x(s)$$

$$U(s) = \left(\frac{(L_1 s + R)(ms^2 + bs)}{K_f} + K_g s\right)x(s)$$

And therefore the transfer function from $U(s)$ to $x(s)$ is

$$\frac{x(s)}{U(s)} = \frac{K_f}{L_1 ms^3 + (Rm + L_1 b)s^2 + (Rb + K_g K_f)s}$$

In the same way the transfer function from $p(s)$ to $x(s)$ is derived.

$$U(s) = 0$$

$$(L_1 s + R)i(s) = -K_g v(s)$$

$$i(s) = \frac{1}{K_f}((ms^2 + bs)x(s) + p(s)A)$$

$$(L_1 s + R)\frac{1}{K_f}((ms^2 + bs)x(s) + p(s)A) = -K_g s x(s)$$

Rearranging gives

$$\frac{x(s)}{p(s)} = -A\frac{L_1 s + R}{L_1 ms^3 + (Rm + L_1 b)s^2 + (Rb + K_g K_f)s}$$

And finally superposition gives

$$x(s) = \frac{K_f}{L_1 ms^3 + (Rm + L_1 b)s^2 + (Rb + K_g K_f)s}U(s) - A\frac{L_1 s + R}{L_1 ms^3 + (Rm + L_1 b)s^2 + (Rb + K_g K_f)s}p(s)$$

5.2.3 Considerations on using this actuator in a lung simulator

The voice coil has several advantages and disadvantages, some due to the design, others due to the fundamental physical workings.

Advantages

- Linear
- Backdrivable
- High acceleration
- Direct drive (no gears etc)
- Low acoustic noise
- High force
- Relatively inexpensive for short strokes

- Low heat production from the few moving parts (little friction)
- High precision

Disadvantages

- Hysteresis due to magnetization
- Heat production from large currents
- Limited range of motions
- Accuracy limited by sensors
- Sensitive to (electrical) noise

For the application in a lung simulator, the advantages outweigh the disadvantages. The most important requirements for the lung simulator, listed in the chapter 'Preferences and Requirements' match the advantages named above: linear, backdrivable, high force and high acceleration.

5.3 Spiral actuator

The overcome the problems of servomotors, T. Kominami and Y. Fujimoto together with several other researchers are developing a spiral direct drive linear actuator and published results in [**24**], [**25**], [**26**], [**27**], [**28**]. In this section their design is analyzed for the use in a lung simulator.

5.3.1 Topology

The basic inner workings are similar to the 'moving coil' concept described in [**25**]: a spiral iron mover fitted with permanent magnets and 3-phase stator coils. Figure 5.7 depicts a CAD model of the design. The spiral mover in Figure 5.7(b) turns and moves forward when a magnetic field is induced in the 3-phase windings, as depicted in [**27**].

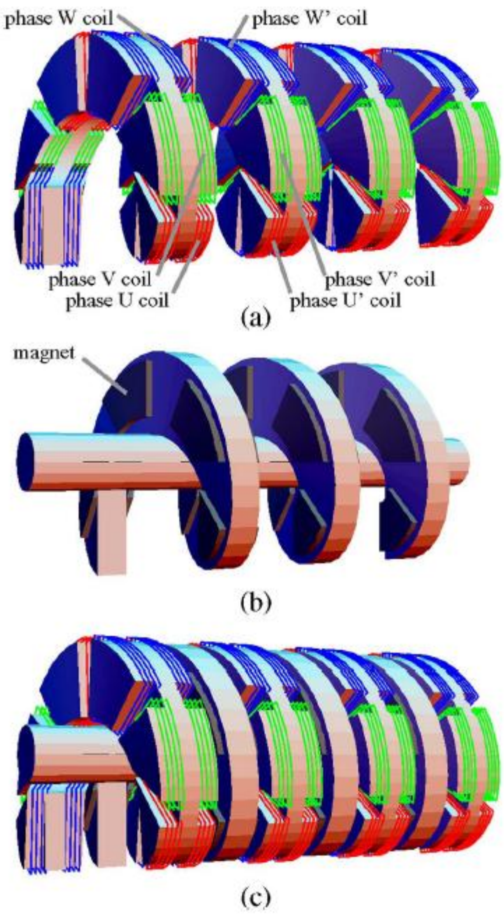

Figure 5.7 – Preliminary structure of a spiral motor, from [29].

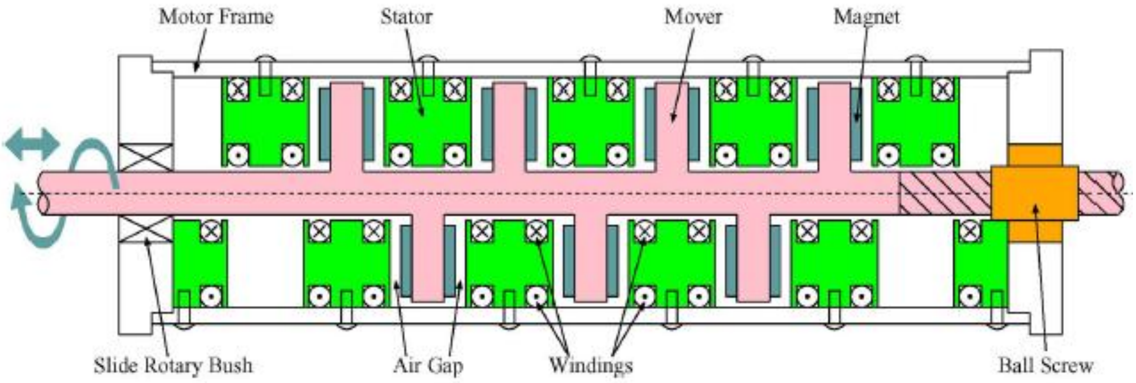

Figure 5.8 - Spiral motor with ball screw to make air gap-control superfluous, [29]

These 3-phase windings are blue, green and red. Aligning them in the axial direction maximizes flux coupling.

5.3.2 Mathematical Model

5.3.2.1 *Nomenclature*

Symbol	Definition
K_f	Thrust-force constant
p	Number of pole pairs per 360◦ electric angular displacement.
q	Number of layers.
n	Number of turns of windings.
S	Gap area per 360° mechanical angle displacement.
μ_0	Permeability in vacuum.
$c(\theta)$	Spatial distribution for magnetomotive force of a permanent magnet.
k	Fundamental Fourier component of $c(\theta)$.
I_m	Magnetomotive force of a permanent magnet.
l_p	Lead length of screw
l	Nominal gap between the mover iron and the stator.

5.3.2.2 *Model*

5.3.2.2.1 Current – thrust force relationship

In [**29**] it is shown that this actuator has a linear current-thrust force relation:

$$F = K_f i$$

where

$$K_f = \frac{2\pi pqnS\mu_0 kI_m}{l_p l}$$

Because this actuator can be modelled as an LTI system, all non-linearity's due to temperature, hysteresis etc., are negligible, it allows for good linear control.

5.3.2.2.2 An electrical equivalent model

Looking at Figure 5.7 every coil can be modelled as follows:

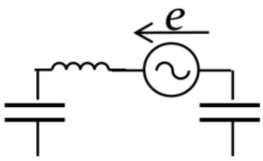

Figure 5.9 - Electrical equivalent model of a coil

In this model, every coil experiences back-emf and a capacitance to the coils on either side.

The three colour windings (blue green and red) are at 3 different phases, $\frac{j2\pi}{3}$ apart, and every 'colour' has a series wire resistance. The total model then looks like this:

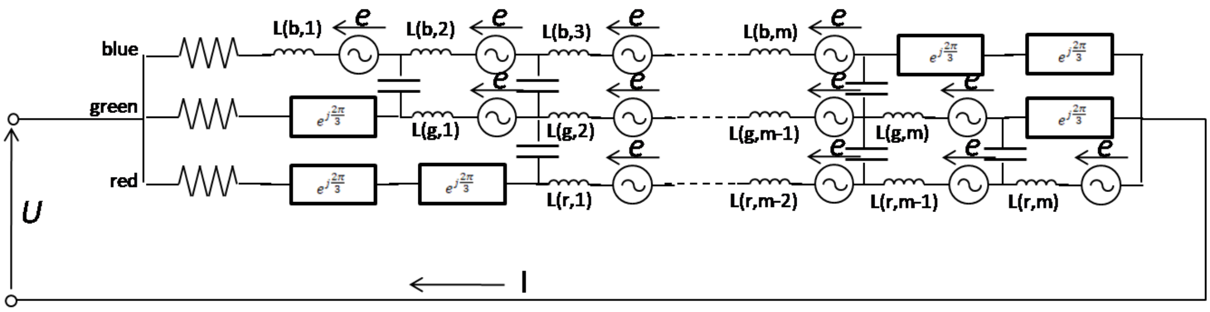

Figure 5.10 - Electrical equivalent model of the spiral actuator

Given that this actuator operates at low frequencies, the displacement current between adjacent coils is neglected. Also, flux coupling between coils is mainly with coils in series and the simplified system looks like:

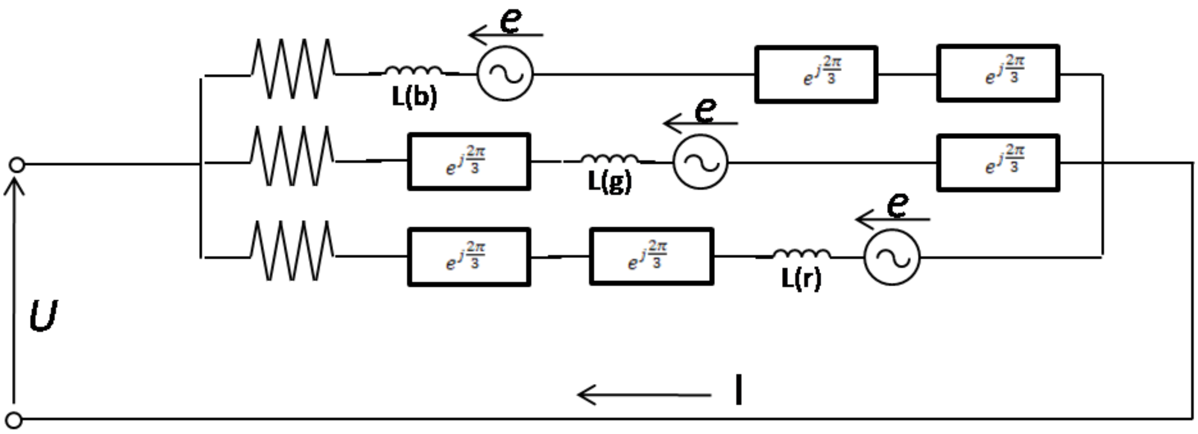

Figure 5.11 - Simplified electrical equivalent model of the spiral actuator

Another way to draw this system is in a Y or Δ configuration; the delays in the system could then be left out.

5.3.3 Considerations on using this actuator in a lung simulator

The positive aspect of this actuator is that it's inherently linear. Also, it promises to have a high thrust force and longer stroke than voice coils, due to its mechanical design. Even though the same principle, the Lorentz force / Lenz' law, is used. Given the design of the present generation of lung simulators, the implementation could be easy, as little changes to the air compartment design have to be made, if the stroke and peak force match that of the brushless dc motor.

On the other hand, the actuator is still under development, and 3rd party evaluation of the concept and design, let alone production, could be several more years ahead. Also, the size and especially weight (43kg) of the prototype described in [**29**], pose a problem in this specific application.

Because this actuator is still under development, it will not be considered any further. Future improvements of the lung simulator, however, could well incorporate this design.

5.4 Linear Permanent Magnet Synchronous Motor

A third candidate is the permanent magnet linear synchronous motor (PMSM), because of its linearity and backdrivability. It's backdrivable for the same reason voice coils are: a PMSM is an electromechanical system without gears and very little friction. One of its uses is the maglev or bullet trains where trains levitate and experience only air resistance. Linear synchronous motors, including the PMSM, and their uses are treated extensively in [**30**].

5.4.1 Topologies

Two topologies are highlighted, though many more designs with their own characteristics exist (described in [**30**]): a design with a moving magnet and one with a moving coil.

5.4.1.1 Moving Magnet

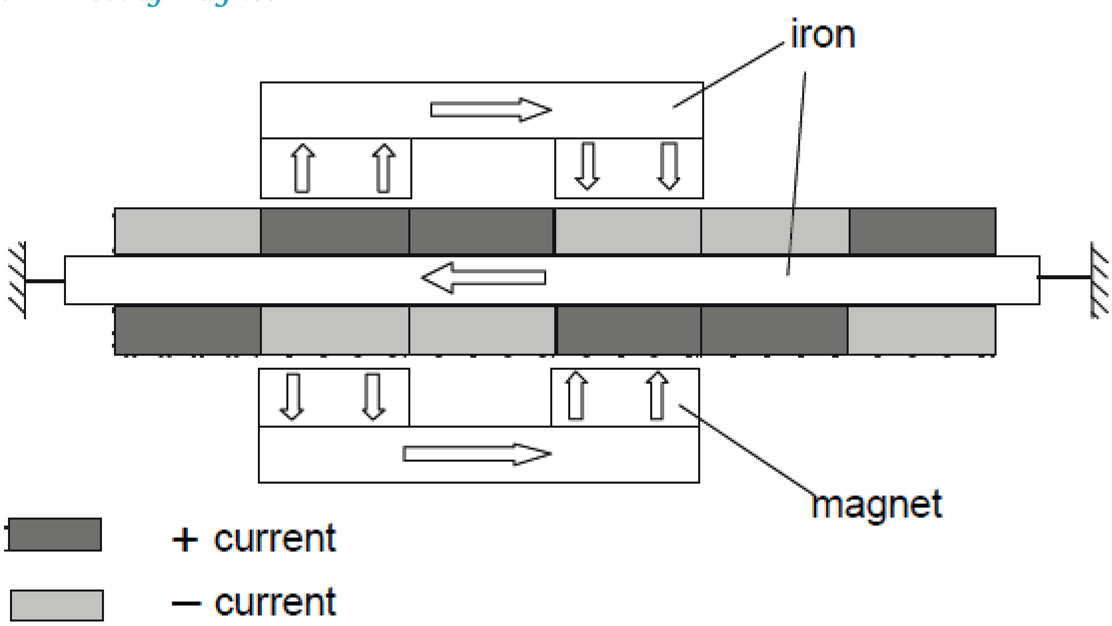

Figure 5.12 - Moving magnet, long stroke.[31]

The design in Figure 5.13 uses the commutating current to position the magnetic slider, though position feedback is necessary. Three advantages are that no moving cable connection is necessary, a high precision accuracy is achievable and it's easy to cool down the actuator. On the other hand, it experiences a lot of iron losses and dissipation of electromagnetic energy.

5.4.1.2 *Moving Coils*

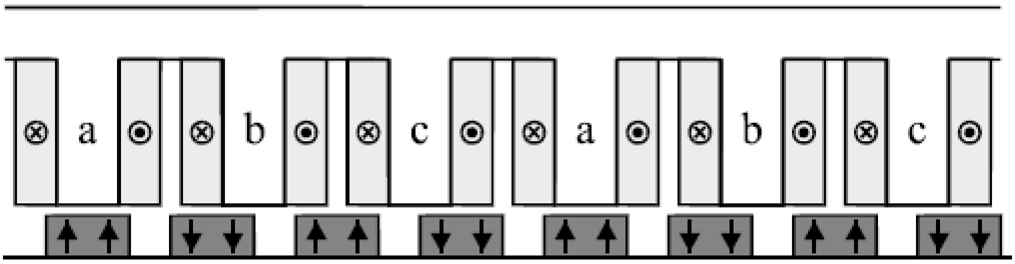

Figure 5.13 - Moving coil, long stroke PMSM. [31]

The design in Figure 5.13 has three phases (labeled a, b and c) in the mover and permanent magnets in the stator. It has a high force density (F/Area) and the accuracy is high, but limited due to cogging and influences from the cable connection to the mover. There is relatively low electromagnetic dissipation, and this design also suffers from iron losses.

5.4.2 Mathematical Model

The theory behind a PMSM is treated extensively in [30].

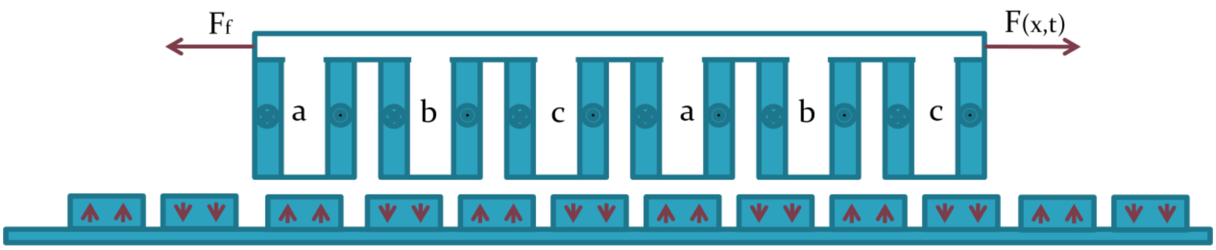

Figure 5.14 - A PMSM with the magnetomotive force and force due to resistance indicated

The force acting on the slider is

$$F(x,t) = \frac{1}{2} F_m \sin\left(\omega t - \frac{\pi}{\tau} x\right)$$

$$F_m = \frac{2 m_1 \sqrt{2}}{\pi p} N_1 I_a k_{\omega 1}$$

Where m_1 is the number of phases, p is the number of pole pairs, N is the number of turns per phase, I_a is the armature phase current, $k_{\omega 1}$ is the winding factor, ω is the angular frequency and τ is the pole pitch.

A simplified mechanical equivalent would look the same as Figure 5.6: a sliding mass with forces acting on the mass and where the mass is connected to the air compartment.

5.4.3 Considerations on using this actuator in a lung simulator

The PMSM has several advantages and disadvantages, some due to the design, others due to the fundamental physical workings.

Advantages

- Linear
- Powerful
- High acceleration
- Long stroke
- Relatively (to a moving magnet topology) low electromagnetic dissipation

Disadvantages

- Cogging
- Limited accuracy
- Position information necessary
- Moving cable connection

The advantages clearly outweigh the disadvantages and this is a well-developed actuator.

5.5 Voice coil: the actuator of choice

5.5.1 Comparison bases

The three actuators are compared on the following bases:

- Backdrivable – whether the piston is easy to move by external forces
- Peak force – whether the necessary force of 350 N can be exerted
- Stroke – whether the device can make a stroke of ~1 dm
- Low speed accuracy – given the simulator mostly moves at low speeds, the accuracy is assessed.
- Robustness – whether the mean time to failure is high; the main factor in grading robustness is whether any connection wires are moving, which is a weak spot.
- Acceleration – whether the actuator can make a sufficient acceleration to simulate different lung pathologies
- Development – the development status is assessed
- Size – whether the actuator is suitably sized for this application

The actuators are graded for every property in a scale from 1 to 10, with 1 being ‘very bad’ and 10 being ‘excellent’.

5.5.2 Grading table

	Voice Coil	Spiral Motor	PMSM
Backdrivable	8	6	8
Peak force	6	10	8
Stroke	6	8	8
Low speed accuracy	9	6	4
Robustness	6	9	6
Acceleration	9	5	7
Development	7	3	7
Size	6	5	7
Total	**57/80**	**52/80**	**55/80**

5.5.3 The voice coil is the most suitable actuator

The voice coil actuator has the highest score, but not by far. The reason the voice coil is chosen, is because it is a well developed actuator with lots of different varieties on the market. The spiral motor is still in development and maybe even too powerful and too large for this application. The PMSM is not chosen, because of cogging: the accuracy for low speeds is too low.

Also, for simulation purposes the behaviour of the system is more important than the actuator chosen. The voice coil has the most representative and accurate model of the three.

6 Simulation of the voice coil actuators and experimental setup

To verify the conclusions made in chapter 5 about the voice-coil actuator as an alternative to the brushless DC motor in the ASL5000, the voice coil is simulated. To do this, the behavior of the actuator is modeled in MATLAB.

6.1 Bode plot analysis of the voice coil

For the simulation of the motor the transfer function of the voice-coil derived in chapter 5 is used:

$$x(s) = \frac{K_f}{L_1 m s^3 + (Rm + L_1 b)s^2 + (Rb + K_g K_f)s} U(s) - A \frac{L_1 s + R}{L_1 m s^3 + (Rm + L_1 b)s^2 + (Rb + K_g K_f)s} p(s)$$

For the simulation, parameters in Appendix E are used.

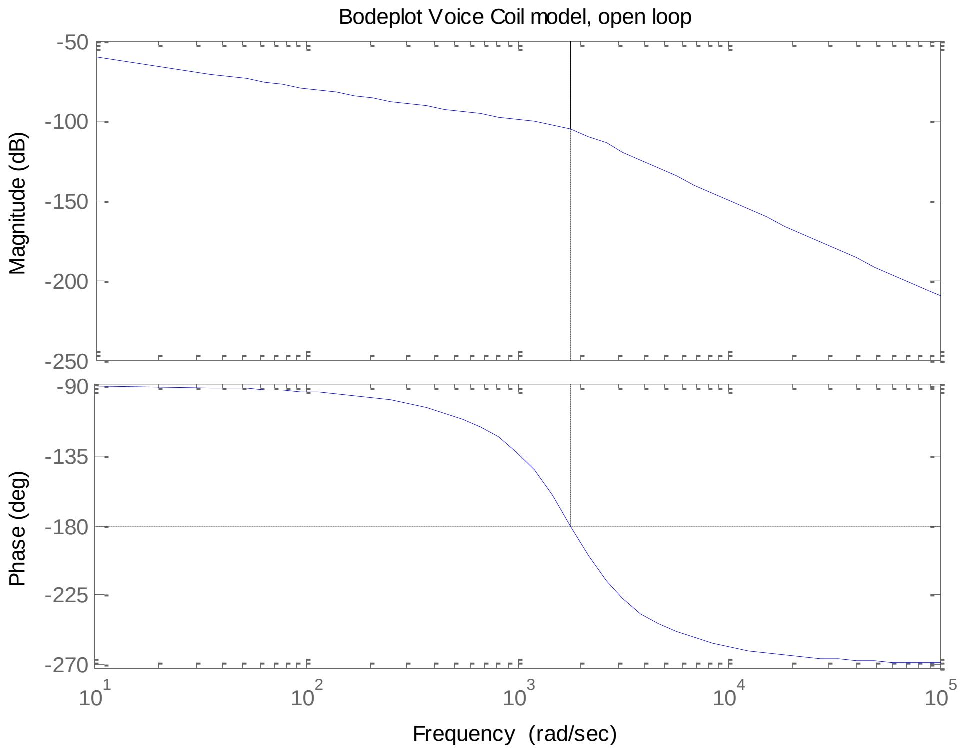

Figure 6.1 - Bode plot of a voice coil, without controller

The Bode plot of the voice coil is depicted in Figure 6.1.

There is a significant damping in the frequeny range that are interesting for this project (the low frequencies). This requires a very large input voltage to lead the piston to move. Due to presence of a pole in 0 it can be concluded that the Phase Margin (PM) is 90 degrees, which requires no improvements. The gain margin (GM) is 106 dB.

6.2 Controller design

The requirements of the actuator are :

- rise time ~0.15 sec
- no overshoot

To reach these requirements P-control is sufficient with a gain of 1200.

Such a large gain in this type of system (the same as in Figure 3.4) is not practically achievable because it leads to very large input voltages to the voice coil. In Figure 6.2 the necessary input voltage is depicted.

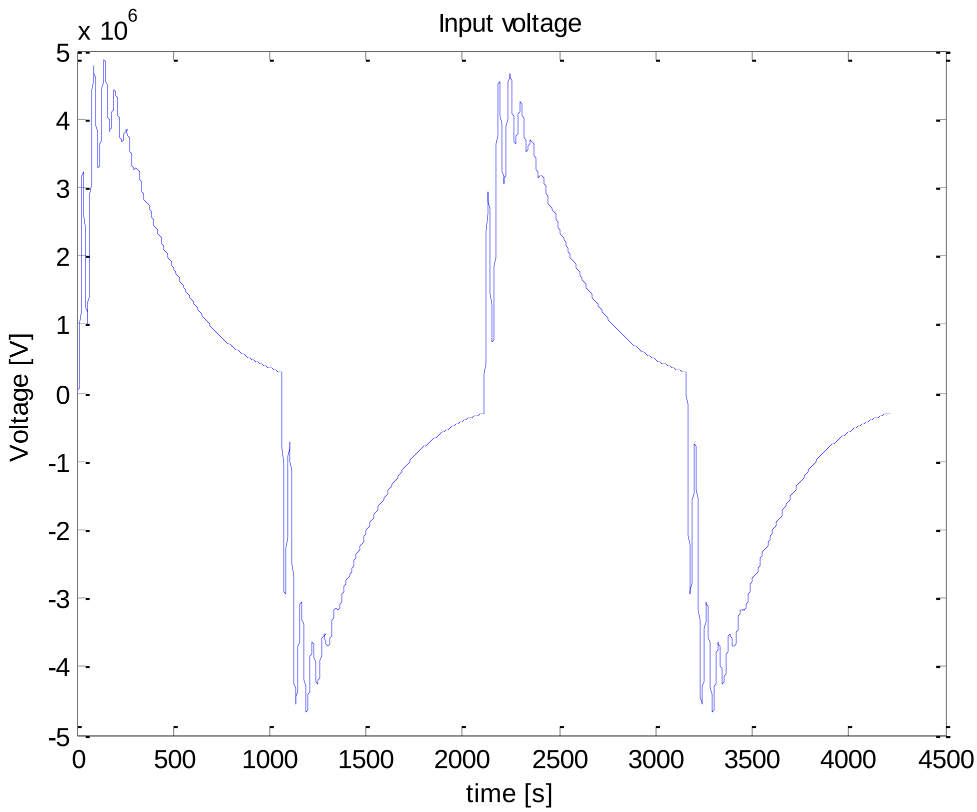

Figure 6.2 - Input voltage for the voice coil when used in direct position regulation.

It's clear that megavolts are not realistic, so the system has to be designed differently.

6.3 A novel system design using inherent backdrivability of the actuator.

To make optimal use of the backdrivability, the voice coil should only change the position due to this backdrivability when it differs from the position that would follow from the lung model, rather than forcing a previously specified position and reject disturbances from the internal pressure.

Figure 6.3 depicts the design proposed.

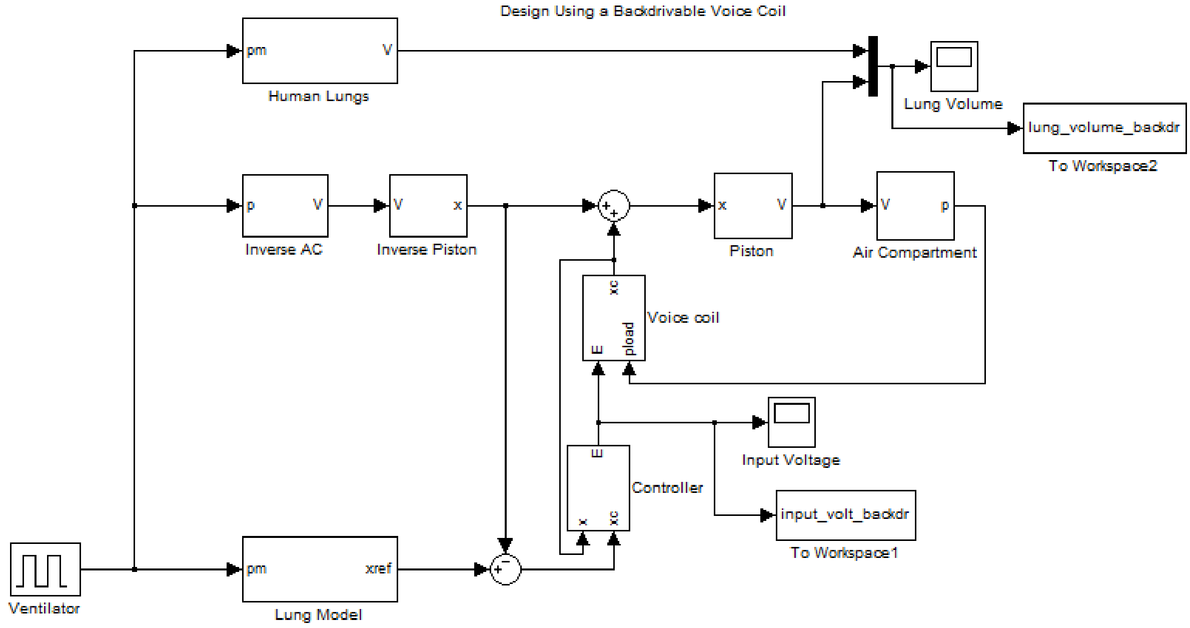

Figure 6.3 - Design of a lung simulator making optimal use of the backdrivability of the voice coil.

Experimenting with this design shows that lung pathologies that were impossible with the non-backdrivable BLDC are accurately simulated with this novel system, as depicted in Figure 6.4.

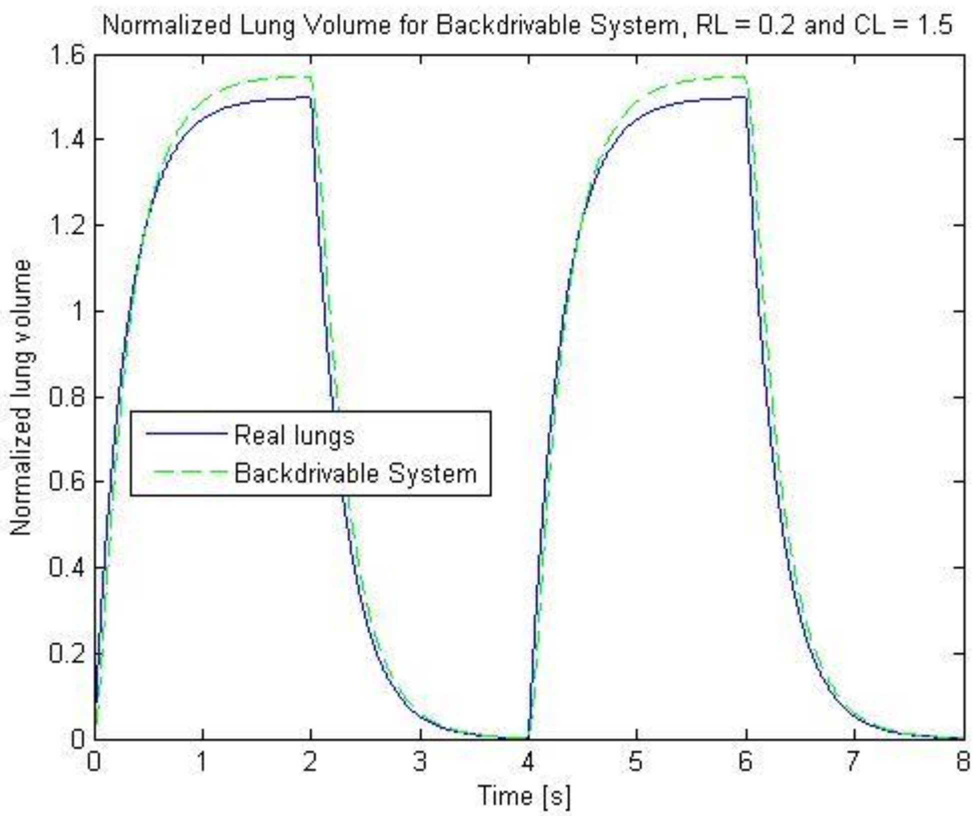

Figure 6.4 - Lung volume for ventilated lungs using the novel system.

Experimenting with the simulation also shows that the difference between the real lung volume and the simulated one is a function of the gain of the controller.

When using the same controller for the voice coil as in the previous system, the input voltages are much more realistic in the backdrivable design than in the previous one, as follows from Figure 6.5.

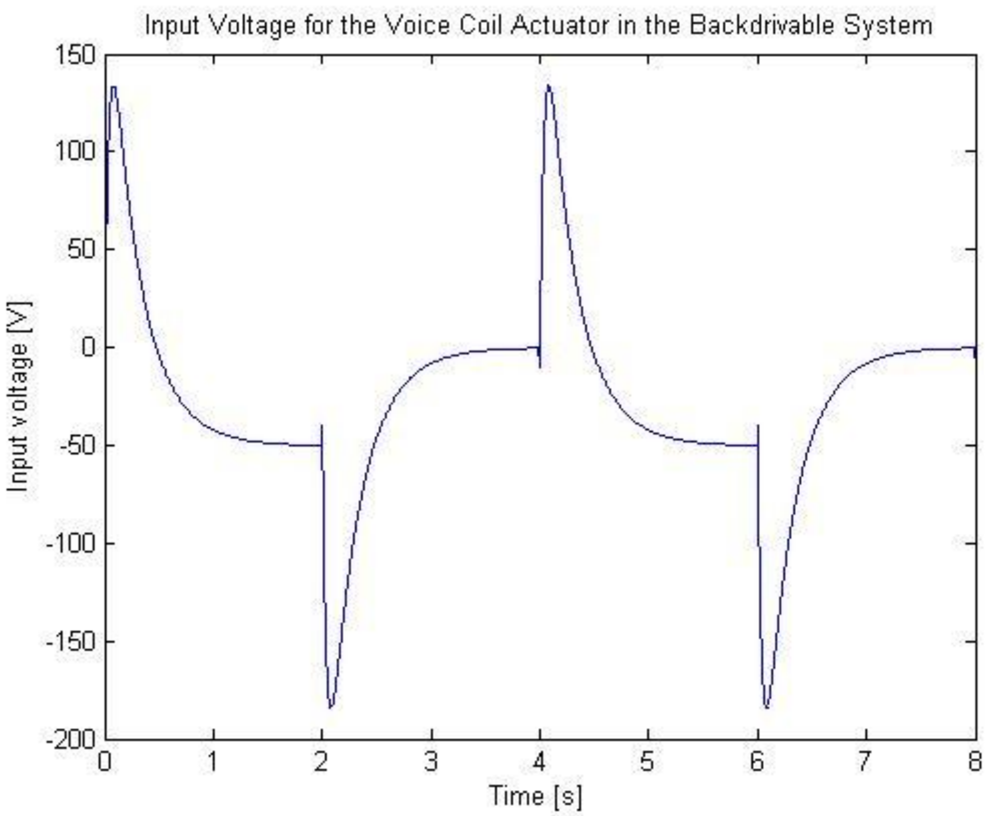

Figure 6.5 - Input Voltage for the voice coil actuator.

7 Conclusion

The question was whether an actuator that responds well to external influences (i.e. an actuator that is backdrivable) could solve instability problems that the current generation of lung simulators experiences.

Backdrivability is indeed able to solve these problems.

The goal of this research project is to improve the current generations of the lung simulators. In this report the driving actuator of the system is considered.

7.1 Some lung pathologies cannot be simulated in a lung simulator with a non-backdrivable actuator

It can be shown in simulations that for certain lung pathologies the system with a brushless DC actuator becomes unstable.

Hypothesis: It is the lack of backdrivability in the Brushless DC motor that causes instability.

To verify this hypothesis, three different backdrivable alternative actuators for the current actuator with their corresponding mathematical model are considered with the aim of choosing an actuator that could be used in a simulation to verify the hypothesis:

- Voice coil
- Spiral motor
- Permanent Magnet Linear Synchronous motor

7.2 A voice coil is suitable for simulation and implementation

To compare the behaviours of the back- and non-backdrivable systems, simulations of a voice coil as replacement for the brushless DC motor are performed. From the first round of simulations it is concluded that the current system is not suitable for voice coil, because the old setup causes input voltages to the voice coil in the order of megavolts. Therefore, another system is designed for this actuator making optimal use of the voice coil's backdrivability.

7.3 Backdrivability can solve the instability problems

After simulating the system, analysis has shown that the system is stable for different lung parameters for which the system with the old actuator becomes unstable. The next logical step is to design an experimental set-up (described in Appendix C) to test the conclusions made above based on the simulations. Due to a lack of time and technical problems with the setup, the test phase was skipped.

To sum up: the hypothesis that a backdrivable system is more suitable for a lung simulator is show to be true by simulations.

Bibliography

[1] I. Gunawan, E. Muijs, and D. Veljacic, "Hardware of the Artificial Respiratory System - Improving and Stabilizing the Lung Simulator," Delft University of Technology, Delft, 2010.

[2] L. Gregoire, *Functionele Anatomie van de Mens*. Leiden, The Netherlands: Spruyt, Van Mantgem & De Does BV, 1990.

[3] A. van het Groenewoud and A. Starreveld-Zimmerman, *Groot Medisch Handboek*. Amsterdam, The Netherlands: Jacob van Campen, 1974.

[4] F. H. C. De Jongh, *Ventilation Modelling of the Human Lung*. Delft, The Netherlands: Delft University of Technology, Faculty of Aerospace Engineering, 1995.

[5] National Heart Lung and Blood Institute. (2010, may) How the Lungs Work. [Online]. http://www.nhlbi.nih.gov/health/dci/Diseases/hlw/hlw_respsys.html

[6] J. W. Chien, D.K. Madtes, and J.G Clark. (2005, 17) Nature. [Online]. http://www.nature.com/bmt/journal/v35/n5/full/1704783a.html

[7] R. Babuska, Computer-Controlled Mechatronic Simulation of the Human Respiratory System, 2010, Handout from Professor Babuska with details on the assignment.

[8] J. T. Sharp, J. P. Henry, S. K. Sweany, W. R. Meadows, and R. J. Pietras, "Total Respiratory Inertance and Its Gas and Tissue Components in Normal and Obese Med," *Journal of Clinical Investigation*, vol. 43, no. 3, pp. 503-509, 1964.

[9] S. Mesic, R. Babuska, H. Hoogsteden, and A. Verbraak, "Computer-Controlled Mechanical Simulation of the Artificially Ventilated Human Respiratory System," *IEEE Transactions on Biomedical Engineering*, vol. 50, no. 6, pp. 731-743, June 2003.

[10] W. Bolton, *Mechatronics: Electronic Control Systems in Mechanical Engineering*. United Kingdom: Longman Sc & Tech, 1996.

[11] P. Pillay and R. Krishnan, "Application Characteristics of Permanent Magnet Synchronous and Brusheless DC Motors for Servo Drives," *IEEE Transactions on Industry Applications*, vol. 21, no. 5, pp. 986-996, September/October 1991.

[12] A. S. O. Al-Mashakbeh, "Proportional Integral and Derivative Control of Brushless DC Motor," *European Journal of Scientific Research*, vol. 35, no. 2, pp. 198-203, 2009.

[13] G. F. Franklin, J. David Powell, and A. Emami-Naeini, *Feedback Control of Dynamic Systems*, 5th ed., V. O'Brien, D. A. George, and C. Little, Eds. Upper Saddle River, United States of Americ, New Jersey: Pearson Prentice Hall;, 2009.

[14] R. Perez-Castillejos et al., "The Use of Ferrofluids in Micromechanics," *Sensors and*

Actuators, no. 84, pp. 176-180, November 2000.

[15] F. Schneider, D. Hohlfeld, and U. Wallrabe, "Miniaturized Electromagnetic Ferrofluid Actuator," in *International Conference on New Actuators*, Bremen, Germany, 2006, pp. 289-292.

[16] G. Magnac et al. (2008, July) Cedrat.com. [Online]. http://www.cedrat.com/fileadmin/user_upload/cedrat_groupe/Publications/Publications/2007/09/LDIA2007_Moving_Coil_or_Iron_Controllable_Actuators_01.pdf

[17] R. Clarke. (2004, Mar.) University of Surrey, UK. [Online]. http://info.ee.surrey.ac.uk/Workshop/advice/coils/force.html

[18] Zac Mullet Engineering Services. (2010, May) Mechatronics. [Online]. http://www.zmeng.com.au/mechatronics/2D-haptic-interface-voice-coil-motor.png

[19] M.J. Hoeijmakers, *Elektrische Omzettingen*. Delft: VSSD, 2007.

[20] University of Technology, Sydney. (2000, February) Scribd.com. [Online]. http://www.scribd.com/doc/29878596/Voice-Coil-Motors

[21] P.A. Tipler and G. Mosca, *Physics For Scientists and Engineers*, 6th ed. New York, USA: S.F. Brennan, 2008.

[22] F. Baronti et al., "Voice coil actuators: From model and simulation to automotive application," in *IECON '09. 35th Annual Conference of IEEE Industrial Electronics, 2009.*, 2009, pp. 1805-1810.

[23] A. Moser, "Shorted Turn Effects in Rotary Voice Coil Actuators," *IEEE Transactions on Magnetics*, vol. 32, no. 3, pp. 1736-1742, May 1996.

[24] T. Kominami and Y. Fujimoto, "Dynamic model and control of six-phase spiral motor," in *The 8th IEEE International Workshop on Advanced Motion Control, 2004. AMC '04.*, 2004, pp. 629-633.

[25] T. Kominami and Y. Fujimoto, "Development of a Spirally-Shaped Linear Actuator," in *Industry Applications Society Annual Meeting, 2008. IAS '08. IEEE*, Oct. 2008, pp. pp.1-5, 5-9.

[26] T. Kominami and Y. Fujimoto, "Dynamic model and control of six-phase spiral motor," in *The 8th IEEE International Workshop on Advanced Motion Control, 2004. AMC '04.*, 2004, pp. 629- 633.

[27] T. Kominami and Y. Fujimoto, "Magnetic levitation control and spiral-linear transformation system for spiral motor," in *9th IEEE International Workshop on Advanced Motion Control, 2006.*, 2006, pp. 529-534.

[28] Y. Fujimoto, I. A. Smadi, H. Omori, K. Suzuki, and H. Hamada, "Modeling and Control of a High-thrust Direct-drive Spiral Motor," in *Proceedings if the IEEJ International Power Electronics Conference (IPEC), 2010*, 201.

[29] Y. Fujimoto, T. Kominami, and H. Hamada, "Development and Analysis of a High Thrust Force Direct-Drive Linear Actuator," *IEEE Transactions on Industrial Electronics*, vol. 56, no. 5, May 2009.

[30] J. F. Gieras and Z. J. Piech, *Linear Synchronous Motors - Transportation and Automation Systems*. Florida, United States of America: CRC Press LLC, 2000.

[31] H. Polinder, Electromechanics in Mechatronic Systems, 2010, Lecture Slide from the ET4245ME course at Delft University.

[32] A. F. M. Verbraak, *Modelling and Data Processing in Pulmonary Function*. Rotterdam, The Netherlands: Erasmus Universiteit Rotterdam, Faculty of Medicine, 1998.

[33] D. Rutter. (2010, May) Rare earth magnets for fun and profit. [Online]. http://www.dansdata.com/images/magnets/voicecoil440.jpg

[34] IngMar Medical. (2010, May) IngMar Medical. [Online]. http://www.ingmarmed.com/

Table of Figures

Appendix A: Minutes of the interview at the Erasmus Medical Centre

Date: May 3rd, 2010 (ErasmusMC)

Attendants:

- Ine Gunawan (secretary), Dejan Veljacic, Anton Delawari (TU Delft)
- Dr. Henk Stam, Wim Holland, Ton Verbraak (Erasmus Medical Centre (EMC))

Minutes:

EMC's applications for lung simulators; measuring:

- Diffusion through lung walls.
- Vital capacity/ max flow/ volume test.
- Narrowing in smaller airways (so-called 'FEV1').
- Perfusion of the lungs.

Requirements

- Device has to have a flow of at least 15 litres/s.
- Residue volume of the lungs (1-2 litres) is included in the cylinder.
- Smaller piston means a more precise volume displacement (due to the longer stroke).
- EMC's current lung simulator's acceleration is 200 litre/s^2.
- Size of the piston ⇔ stroke ⇔ velocity.
- Safety. There's a powerful motor involved:
    - Pressure safety for patients in case the device is used as ventilator
    - For the device itself in case of overpressure or underpressure: it can explode or implode.
    - For other connected devices: it cannot hurt other equipment in case of failure.
    - In case the devise works with gasses, the hoses should be impermeable.

Appendix B: The interview with Mr. T. Verbraak on the ethical aspects of engineering in the medical business (Dutch)

Inleiding

Naarmate onze leven steeds meer van de techniek afhangt, worden de ethische aspecten van de techniek en gevolgen hiervan belangrijker. Dat eist van toekomstige ingenieurs dat ze tijdens hun studie ook aan de ethische vragen die kleven aan hun ontwerpen tijd besteden.

Echter, het is niet voldoende, omdat als student men geen ervaring heeft in het bedrijfsleven waardoor sommige knelpunten worden niet gezien. Om dat te voorkomen, is het verstandig om iemand uit de zelfde tak van het bedrijfsleven te interviewen.

Wie zijn wij: Anton Delawari en Reinier Doelman. Voor het halen van de Bachelor Elektrotechniek bekijken we verschillende alternatieven voor de aandrijving van een longsimulator.
Wie hebben wij geïnterviewd: Ton Verbraak, recent gepromoveerd op het ontwerp van een longsimulator en tegenwoordig gepensioneerd.

Dit interview is als volgd opgebouwd: we poneren eerst de vraag die we gesteld hebben, dan een citaat uit het antwoord, en daarna voegen wij ons commentaar daaraantoe. Na het interview analyseren we de antwoorden aan de hand van ethische theoriën.

Interview

1. Wat vindt u van het idee achter dit interview?

"Als eerste opmerking denk ik dat jullie met name jullie eigen mening (…) naar voren moeten brengen. Veel antwoorden kunnen anders worden ingevuld al naar gelang welke maatschappijvisie men heeft. Momenteel kunnen we dagelijks de verschillende oplossingen van de politici vernemen al naar gelang de politieke kleur."

2. Wat vindt u er van dat veel bedrijven in de medische sector commerciële doelen hebben en niet non-profit zijn? Vindt u het ethisch verantwoord (veel) geld te verdienen met gezondheid?

"Veel geld is niet goed. In een gezonde bedrijfstak is het belangrijk dat men ook redelijk (marktconform) verdiend. Het is geen vrijblijvend vrijwilligerswerk."

Extreme commercialisatie van de zorgsector vindt meneer Verbraak heel negatief. Hiermee kan men verstaan dat de zorg ook moet streven naar zorg en niet heel blind op winst uit moet zijn. Tegelijkertijd geeft hij nadruk dat deze sector niet non-profit moet zijn. Dit zou namelijk veel talent aan de kant zetten, omdat niet iedereen bereid is om mensen vrijwillig te helpen.

3. Bent u in uw carriere ooit tegengekomen dat een medisch/technisch ontwerp om financiele redenen aan kwaliteit moest inboeten? Wat vond u daarvan, of wat zou uw mening daarover zijn?

" Voor elke toepassing is men veelal in concurentie met andere (ook) belangrijke projecten. Omdat de bomen niet tot de hemel groeien zal men niet steeds het optimale ontwerp kunnen realiseren."

Het is duidelijk dat een optimaal ontwerp dus heel moeilijk te realiseren is. Waar we over verwonderd zijn is het besef dat het ene medische project ook een concurrent van de andere is. Waar leg je dan prioriteit?

4. De stelling is: met groeiende financiele belangen wordt door grote bedrijven gelobbyd, waardoor niet altijd voor het beste technische (of goedkoopste) ontwerp door ziekenhuizen gekozen wordt. Kunt u hier een mening of oordeel over geven, ook als de geschetste situatie niet het geval is?

"Te veel lobby werk is niet goed. Wel indien het een vorm van adverteren is om de voordelen van het eigen product naar voren te brengen. Overdreven lobbywerk moet de ontvanger afwijzen."

Er is een onderscheid tussen verschillende soorten lobby: één, alleen in de zin van adverteren en twee, wat tegenwoordig gebeurt (dat minder goede producten of diensten het contract aangeboden krijgen door goed werk van een accountmanager). Meneer Verbraak spreekt van een gedoging van de eerste.

5. Hoe bent u omgegaan met veiligheidsrisico's voor derden van de ontwerpen die u maakte?

"Neem steeds in ogenschouw of men ook een van de eigen kinderen hieraan zou bloodstellen."

Een lovenswaardige houding, het sluit aan bij de theorie van Levinas en die van Kant.

6. Wat vindt u ervan dat in de globaliserende samenleving steeds vaker productie in landen plaatsvindt waar werknemers niet tegen werkgevers beschermd worden (denkt u aan kinderarbeid, extreem lange werkdagen etc.)?

"Men moet hier allert op zijn. Met name als consument kan men hier sturing aan geven."

Het is alleen in de handen van de consument om de schone achtergrond van de productie te eisen van de producent. Als de consument voorkeur geeft aan de goedkope producten dan zou er grotere kans zijn voor kinderarbeid. Van een verantwoordilijkheid vanuit de ontwerper wordt niet gesproken. Invloed van de consument is echter ook veel groter.

7. Kunt u uw mening geven over beloningsverschillen tussen doktoren, verplegend personeel en technische ingenieurs in de medische wereld? Wat zou u doen als u de verschillen zou kunnen bepalen?

"Uiteraard zijn veel uitwassen in de salariering van doktoren niet goed te keuren. Ik denk dat met name in de acdemische omgeving zal meevalen. In de perifere ziekenuizen zijn te verschillen bij sommige specialismen te groot."

Volgens meneer Verbraak vallen de verschillen in de universiteit waarin hij heeft gewerkt mee; de oorzaak is de academische omgeving die minder snel naar hoge salarissen streeft. Maar de onzinnelijke verschillen in de "perifere ziekenhuizen" zijn niet gewaardeerd, want alleen door de samenwerking tussen alle lagen van personeel in de ziekenhuizen worden patiënten op het gewenste niveau behandeld.

8. Weet u iets van ethische (gedrags)codes voor ingenieurs in de medische wereld? Wat zou naar uw mening er zeker in moeten staan?

"Voor zover mij bekend is er geen expliciete gedragscode. Wel wordt hieraan aandacht besteed bij de opleiding tot Klinisch Fysicus[5] *en aan de opleiding tot medisch ingenieur aan de TU-Eindhoven*[6,7]*."*

Evaluatie

Meneer Verbraak heeft heel lang gewerkt in de voor ons relevante sector. Het is duidelijk te zien dat hij standpunten hierover heeft. Echter hij wil die niet zomaar kwijt, omdat volgens hem studenten zelf zich deze vragen bewust moeten stellen.

Gevolgenethiek, het utilisme van Bentham en Mill

Bij een aantal vragen is duidelijk te zien dat meneer Verbraak een oordeel heeft gevormd die zijn oorsprong heeft in de gevolgenethiek.

Bij vraag 2, over commerciële doelstellingen in de zorgsector, leent deze theorie zich bij uitstek: een kosten-baten-analyse is snel gemaakt. Baten vallen voornamelijk toe aan degene die het commerciële doel nastreeft: extra inkomsten of meevallende uitgaven worden makkelijk als positief bedrijfsresultaat genoteerd, en minder makkelijk geherinvesteerd in de kwaliteit van de zorg. De 'kosten' in deze analyse daarentegen vallen toe aan patiënten die slechter worden behandeld. Dit kan negatieve gevolgen hebben, zelf de dood. Maar andersom is, zeker omdat we het over de zorg hebben, de dood niet per se het gevolg van slechte kwaliteit zorg. Het punt dat ik hier wil maken, is dat de meetbaarheid te wensen overlaat. Natuurlijk is een lage kwaliteit van zorg onwenselijk.

Een andere interessant antwoord was die op vraag 3. De afweging hier is dat precies het credo van utilisme: doordat een bedrijf natuurlijk een beperking heeft op kosten, en een apparaat dat perfect werkt zeker te veel kost om te verkopen, kan er gekozen worden om zoveel mogelijk geluk voor zoveel mogelijk mensen te creëeren.

Plichtethiek, de universaliseringstheorie van Kant

Een algemene wet voor de situatie van vraag 4 die zou voorschrijven dat men zich moet laten beinvloeden door een extreme hoeveelheid lobby (op het corrupte af) zou funest zijn voor de zorg (en niet alleen voor de zorg natuurlijk). Het is duidelijk dat lobby weinig tot geen invloed mag hebben. Maar wat is toelaatbaar? Waar ligt de grens tusse het informeren van artsen enerzijds en het overdreven beïnvloeden van de keuze anderzijds? Wellicht dat een beroepscode zich hierover kan uitspreken.

Er zijn twee manieren om het antwoord op vraag 5 te analyseren: vanuit de plichtethiek en de verantwoordelijkheidsethiek, de laatste wordt onder dat kopje besproken. In vraag 5 wordt, zo

[5] www.nvkf.nl
[6] www.medischetechnologie.nl
[7] www.rathenau.nl

is te beargumenteren, mensen als doel en niet als middel gezien, omdat een vereenzelviging met eigen kinderen dat effect heeft.

Bij vraag 6 wordt de verantwoordelijkheid gelegd bij de consument, die wordt geacht vanuit normen te handelen; een rol voor de ontwerper lijkt nauwelijks weggelegd. Normen sluiten ook aan bij kant universaliseringstheorie.

De deugdenethiek van McIntyre

Beroepscodes sluiten nauw aan bij de deugdenethiek van McIntyre. We vinden het verwonderlijk dat er nooit een expliciete gedragscode speciefiek voor medisch ingenieurs is opgesteld: doktoren kennen hun verantwoordelijkheden, maar tegenwoordig kunnen fouten door ingenieurs en wetenschappers grotere consequenties dragen. Het Koninklijk Instituut van Ingenieurs, KIVI NIRIA, heeft een gedragscode.[8] Ook de Institute for Electrical and Electronics Engineers heeft een gedragscode gepubliceerd.[9]

De verantwoordelijkheidsethiek van Levinas

Zoals al eerder vermeld kan het antwoord op vraag 5 ook uitgelegd worden in het licht van de verantwoordelijkheidsethiek. Je wordt gevraagd voor anderen dezelfde betrokkenheid te voelen als voor je kinderen, en vanuit die betrokkenheid te handelen.

Ook bij de uiteenlopende salariëring van vraag 7 kan opgemerkt worden dat er verantwoordelijkheidsethiek verscholen ligt. In een academische omgeving lijkt er meer verdraagzaamheid te bestaan die gelijke belonging stimuleert. Is dit vanuit een saamhorigheid of komt dit voort uit het feit dat men in de publieke sector werkt en beloning van bovenaf wordt opgelegd, of misschien allebei?

---

[8] Directe link: http://www.kiviniria.net/CM/PAG000002804/Gedragscode-2006.html
[9] Directe link: http://www.ieee.org/membership_services/membership/ethics_code.html

Appendix C: Experimental setup

To verify the results of the simulations, two experiments are necessary: an experiment testing the brushless DC motor and an experiment with a voice coil to compare the two. First, an experiment with the brushless DC motor is described; second, an experiment with a voice coil is described.

Experiment with a brushless DC motor.

Set up

The set up is largely provided for by IngMar Medical. This setup is the core of the ASL5000 Lung Simulator: an air compartment with piston, screw and a brushless dc motor. The motor decoder and pressure sensor are connected to a PC with MATLAB installed.

[plaatje (foto?) setup]

Test

Different inputs are sent to the decoder for different lung models (see section 2.4) and the behaviour of the system is observed by logging the following variables:

- DC current through the motor,
- Pressure in the air compartment from the pressure sensor,
- Position/angle of the screw.

The results of the experiments should verify the simulation results: for some specific lung models the system is unstable. It's expected that the undesirable oscillations are caused by the delay in the feedback loop.

Experiment with a voice coil.

Set up

For an ideal set up for the experiments with voice-coil, the air compartment has to be replaced due to the small volume. As mentioned in the Preferences and Requirements in chapter 4, the internal volume is required to be at least 10 litres. To keep the stroke of the motor not too long, the piston area is required to be significantly large. This would cause a large air mass per dm displacement of the piston. Thus, a compromise has to be made between stroke and the piston area for a specific voice coil actuator. The choice of voice coil is also a compromise between stroke and the force. For the ideal situation stroke has to be about 200mm and with a peak force of 350N. In the case a voice coil with such of performance doesn't exist or is not commercially viable, several low-force voice coils with sufficient stroke could to be placed in parallel. The behaviour of several parallel connected voice-coils needs further investigation, though. To eliminate undesired friction, it's best to connect the voice coil directly to the piston (Figure 0.1).

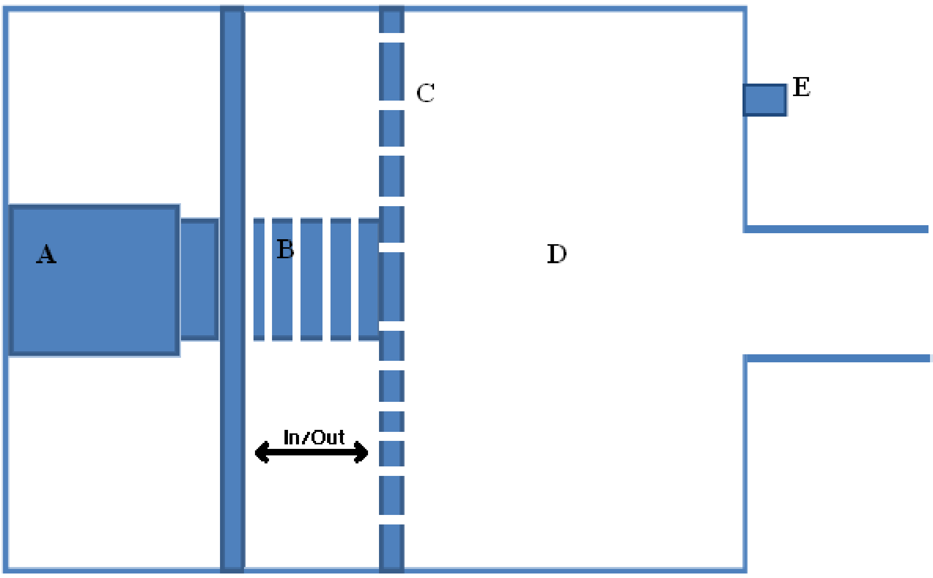

Figure 0.1 - Schematic setup for a lung simulator with a voice coil and an air compartment with (a) the voice coil, (b) a rod, (c) the piston, (d) the air compartment and (e) a sensor for the internal pressure.

In case for the experiment the air compartment from IngMar Medical is used in the experiment with a voice coil, the brushless DC motor has to be demounted. At the end of the screw the voice coil is to be placed and fixed to the construction (Figure 0.2).

Test

The same tests as for the BLDC have to be performed. The expected results are that for different lung parameters the system doesn't become unstable and doesn't make any unexpected oscillations. It's expected that the simulations in section 34 and the experiments are roughly similar.

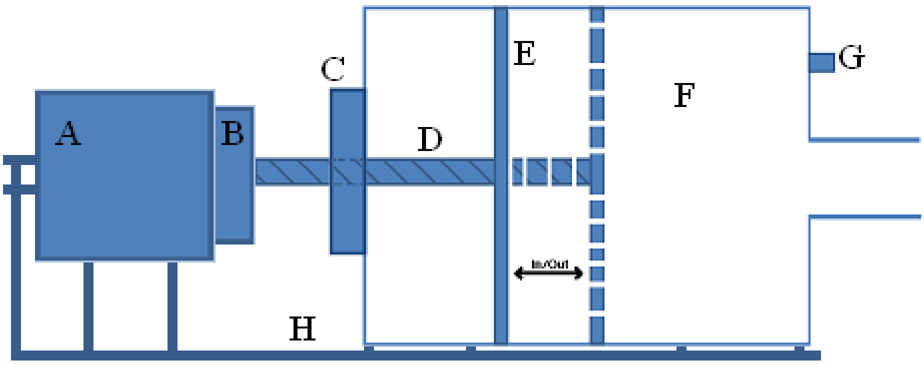

Figure 0.2 - Schematic setup for a voice coil attached to the ASL5000. (a) the voice coil frame, (b) the moving coil, (c) the (removed) dc motor, (d) the screw, (e) the piston, (f) the air compartment, (g) the sensor for the internal pressure.

Appendix D: Frameless motors series datasheet

Frameless Motors Series:
Build Your Own High Performance Motor

The frameless kit motors are ideal solutions for machine designs that require high performance in small spaces. The kit motors approach allow for direct integration with a mechanical transmission device, eliminating parts that add size and compliance. The use of frameless kit motors result in a smaller more reliable motor package.

When to Use:

- A significant cost savings
- Reduced mechanical complexity
- Greater design flexibility
- High performance in a compact package
- Improved dynamic response and settling
- Minimum motor size per application space
- Low cogging for smooth operation
- Low inertia for high acceleration

Applications:

- Automotive
- Machine Tool
- Material Handling
- Packaging
- Robotics
- Semiconductor

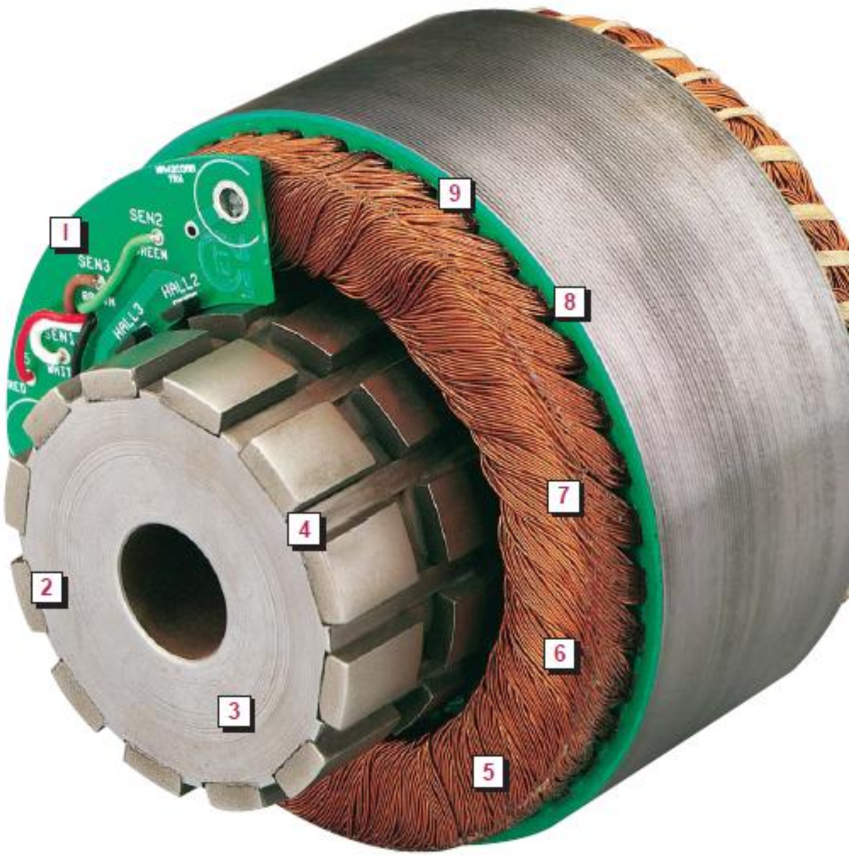

What goes into our Frameless Kit Motors...

Our direct drive brushless kit motors consist of three components:

- The stator and winding
- The rotor with high energy product neodymium magnets
- Hall sensor device for motor commutation

What comes out of our Frameless Kit Motors...

- High Torque - from 0.06 Nm (0.5 in lb) to 9.7 Nm (85.6 in lb)
- High Speeds - up to 50,000 RPM
- Superior Performance - high stiffness and better response
- High Reliability - no mechanical transmission devices (couplings, flanges)
- Compact Design - minimizes product size
- Low Cogging - unique magnetic circuit design decreases cogging
- No RFI-EMI generation

Servo Motors & Drives

1. **Pre-installed Integral Commutation Board**
   with Hall Effects is prealigned for easy assembly. Motor and feedback as integrated unit.
2. **Rare Earth Magnets**
   provide high flux in a small volume, high resistance to thermal demagnetizing
3. **Rotor Assembly**
   for easy mounting directly on the drive shaft with or without keyway.
4. **Machined Grooves**
   to securely lock magnets to rotor and ensures optimized radial location.
5. **Class H Insulation**
   for high temperature operation (up to 155ºC) meeting UL approved requirements.
6. **High Density Copper Winding**
   for low thermal resistance and consistent performance across all motors.
7. **Minimized End Turns**
   to maximize performance. Formed to minimize motor size.
8. **Skewed Laminations**
   with odd slot counts reduce cogging for precise rotary motion with drastically reduced torque ripple even at low speeds.
9. **Optimized Slot Fill**
   for maximum torque-to-size ratio hand inserted to obtain highest slot fill possible maximizing ampere-turns.

Frameless Motors Series:

K032 to K0254 Motors

Performance Specifications (six step/trapezoidal commutation)

Frame Size	Stack Length		Continuous Torque (1) T_c		Peak Torque T_p		Motor Constant K_m		Core Loss P_c	Rotor* Inertia J_m		Electrical Time Constant T_c	Thermal Resistance	Weight Wm	
	(mm)	(in)	(Nm)	(oz in)	(Nm)	(oz in)	(Nm/√W)	(oz in/√W)	W @1kRPM	(gm cm sec²)	(oz in sec²)	(msec)	(°C/W)	(kg)	(oz)
K032025	6.35	0.25	0.044	6.3	0.095	13.5	0.009	1.25	0.03	0.0016	0.000022	0.21	3.44	0.042	1.5
K032050	12.7	0.5	0.08	11.4	0.188	27	0.016	2	0.06	0.0032	0.000045	0.35	3.44	0.068	2.4
K032075	19.05	0.75	0.11	15.7	0.281	40	0.022	3	0.09	0.0048	0.000067	0.44	3.44	0.096	3.4
K032100	25.4	1	0.136	19.4	0.375	54	0.027	4	0.12	0.0064	0.000089	0.5	3.44	0.122	4.3
K032150	38.1	1.5	0.181	25.8	0.544	77.7	0.036	5.15	0.18	0.0096	0.000134	0.6	3.44	0.173	6.1
K032200	50.8	2	0.22	31.1	0.654	93.4	0.044	6.25	0.24	0.013	0.000178	0.66	3.44	0.26	9.2
K032300	76.2	3	0.33	46.5	0.99	139.5	0.054	7.56	0.36	0.0192	0.000268	0.7	3.44	0.36	12.8
K044025	6.35	0.25	0.119	17	0.357	50	0.02	3	0.11	0.0072	0.0001	0.39	2.36	0.085	3
K044050	12.7	0.5	0.214	30.6	0.642	90	0.035	5	0.24	0.014	0.0002	0.62	2.36	0.133	5
K044075	19.05	0.75	0.297	42.4	0.891	127	0.049	7	0.37	0.022	0.0003	0.76	2.36	0.200	7
K044100	25.4	1	0.364	52	1.092	156	0.06	9	0.49	0.03	0.00041	0.89	2.36	0.224	8
K044150	38.1	1.5	0.501	71	1.510	213	0.08	11.4	0.74	0.044	0.00061	1.05	2.36	0.311	11
K044200	50.8	2	0.607	86	1.820	258	0.097	13.8	1.11	0.06	0.00082	1.12	2.36	0.399	14.1
K044300	76.2	3	0.96	136.0	2.88	408	0.13	18.3	1.48	0.088	0.00122	1.3	2.36	0.549	19.4
K064025	6.35	0.25	0.31	44.3	0.93	133	0.048	6.88	0.37	0.046	0.00064	0.59	1.68	0.142	5
K064050	12.7	0.5	0.62	89	1.87	267	0.087	12.48	0.78	0.092	0.00128	0.98	1.68	0.286	10.1
K064075	19.05	0.75	0.85	121.7	2.56	365	0.122	17.44	1.19	0.138	0.00192	1.26	1.68	0.427	15.1
K064100	25.4	1	1.08	154	3.23	462	0.15	21.44	1.6	0.184	0.00256	1.47	1.68	0.572	20.2
K064150	38.1	1.5	1.46	209	4.39	627	0.204	29.12	2.37	0.276	0.00384	1.77	1.68	0.846	30.2
K064200	50.8	2	2.16	308	6.47	924	0.244	34.88	3.23	0.369	0.00512	1.97	1.68	1.129	40.3
K064300	76.2	3	2.91	410	8.73	1,230	0.33	46.6	4.74	0.552	0.00768	2.6	1.68	1.701	60.5
K089050	12.7	0.5	1.307	186.7	3.92	560	0.164	23.36	2.14	0.38	0.00528	1.26	1.02	0.498	17.6
K089075	19.05	0.75	1.96	280	5.88	840	0.235	33.6	3.35	0.576	0.008	1.64	1.02	0.747	26.4
K089100	25.4	1	2.618	374	7.84	1,120	0.283	40.64	4.42	0.792	0.0011	1.92	1.02	0.996	35.2
K089150	38.1	1.5	3.92	560	11.76	1,680	0.381	54.4	6.7	1.15	0.016	2.33	1.02	1.494	52.8
K089200	50.8	2	4.291	613	12.87	1,839	0.466	66.56	8.95	1.51	0.021	2.6	1.02	1.992	70.4
K089300	76.2	3	7.13	1,004	21.4	3,012	0.631	88.9	13.4	2.30	0.032	2.9	1.02	3.00	105.6

(1) = Housed in a motor frame.
Typically an aluminum cylinder with 6.35mm (0.250in) thick walls,
K032, K044 and K064 mounted to a 152mm x 152mm x 12.5 mm (6in x 6in x 0.5in) aluminum plate
K089 mounted to a 203mm x 203mm x 12.5mm (8in x 8in x 0.5in) aluminum plate
* See Engineering Reference page 297 for inertia discussion.

<u>Pole Count</u>
K032 is 4
K044 is 6
K064 is 8
K089 is 12

Frame Size	Stack Length		Continuous Torque (1) T_c		Peak Torque T_p		Motor Constant K_m		Core Loss P_c	Rotor* Inertia J_m		Electrical Time Constant T_c	Thermal Resistance	Weight Wm	
	(mm)	(in)	(Nm)	(oz in)	(Nm)	(oz in)	(Nm/√W)	(oz in/√W)	W@1kRPM	(gm cm sec²)	(oz in sec²)	(msec)	(°C/W)	(kg)	(oz)
K375050	12.7	0.5	1.715	245	5.14	734	0.153	21.8	1.2	0.324	0.0045	1.45	1.02	0.611	21.6
K375075	19.05	0.75	2.401	343	7.19	1,027	0.213	30.4	1.8	0.497	0.0069	1.9	1.02	0.917	32.4
K375100	25.4	1	3.003	429	9	1,286	0.267	38.1	2.4	0.655	0.0091	2.24	1.02	1.095	38.7
K375150	38.1	1.5	4.025	575	12.6	1,723	0.357	51	3.6	1.01	0.014	2.68	1.02	1.554	54.9
K375200	50.8	2	4.935	705	14.82	2,117	0.438	62.6	4.8	1.30	0.018	3.03	1.02	2.02	71.1
K375300	76.2	3	6.69	942	20.1	2,826	0.592	83.4	7.2	2.02	0.028	3.5	1.02	2.94	103.5
K127050	12.7	0.5	3.94	563	11.83	1,690	0.29	41.4	4.7	1.15	0.016	2.38	0.7	1.087	38.4
K127100	25.4	1	6.98	997	21.04	3,006	0.513	73.3	9.6	2.38	0.033	3.7	0.7	1.766	62.4
K127150	38.1	1.5	9.56	1,365	28.66	4,094	0.702	100.3	14.5	3.53	0.049	4.6	0.7	2.355	83.2
K127200	50.8	2	11.75	1,678	35.24	5,034	0.864	123.4	19.4	4.75	0.066	5.23	0.7	2.99	105.6
K127300	76.2	3	16.1	2,263	48.3	6,789	1.18	166.1	29.0	7.06	0.098	6.1	0.7	3.65	147.2
K500050	12.7	0.5	3.05	435	9.14	1,306	0.224	32	1.6	1.15	0.016	2.6	0.7	1.087	38.4
K500100	25.4	1	5.49	784	16.46	2,352	0.403	57.6	3	2.30	0.032	4.5	0.7	1.766	62.4
K500150	38.1	1.5	7.92	1,131	23.76	3,394	0.582	83.2	4.8	3.46	0.048	6	0.7	2.355	83.2
K500200	50.8	2	9.44	1,349	28.32	4,046	0.694	99.2	6.4	4.61	0.064	6.4	0.7	2.988	105.6
K500300	76.2	3	15.4	2,170	46.2	6,510	1.13	159.3	8.6	6.92	0.096	8.0	0.7	4.18	147.2
K178050	12.7	0.5	10.12	1,445	16.18	2,312	0.627	89.6	9.1	4.75	0.066	4.16	0.5	2.4	84.8
K178100	25.4	1	18.06	2,580	28.89	4,127	1.12	160	18.7	9.36	0.13	6.54	0.5	3.71	131.2
K178150	38.1	1.5	24.75	3,535	39.59	5,655	1.534	219	14.4	14.4	0.2	8.15	0.5	4.98	176
K178200	50.8	2	30.7	4,386	49.12	7,017	1.904	272	18.7	18.7	0.26	9.31	0.5	6.34	224
K178300	76.2	3	43.1	6,078	69.0	9,724	2.68	377	28.8	28.8	0.4	12.2	0.5	8.90	313.6
K700050	12.7	0.5	5.05	722	8.09	1,155	0.314	44.8	7.70	7.7	0.107	2.9	0.4	2.4	84.8
K700100	25.4	1	9.57	1,367	15.32	2,188	0.594	84.8	15.4	15.4	0.214	5	0.4	3.71	131.2
K700150	38.1	1.5	13.55	1,935	21.67	3,096	0.84	120	23.2	23.2	0.322	6.8	0.4	4.98	176
K700200	50.8	2	17.52	2,503	28.03	4,004	1.086	155.2	30.9	31	0.429	8.5	0.4	6.34	224
K700300	76.2	3	27.5	3,876	44.0	6,200	1.53	215	46.4	46.4	0.644	10.7	0.4	8.91	313.6
K254050	12.7	0.5	18.78	2,683	30.04	4,292	1.043	149	17.9	17.9	0.248	6.05	0.4	4.48	158.4
K254100	25.4	1	33.92	4,846	54.27	7,753	1.883	269	35.5	35.5	0.493	9.63	0.4	6.79	240
K254150	38.1	1.5	46.84	6,692	74.95	10,707	2.597	371	53.1	53.1	0.738	12.5	0.4	9.056	320
K254200	50.8	2	58.35	8,336	93.37	13,338	3.234	462	71.0	71	0.986	14.7	0.4	11.32	400
K254300	76.2	3	80.9	11,400	129.4	18,240	4.49	632	106.2	106	1.478	18.0	0.4	15.9	560

(1) = Housed in a motor frame. Typically an aluminum cylinder with 6.35mm (0.250in) thick walls,
K375, K127 and K500 mounted to a 305mm x 305mm x 12.5mm (12in x 12in x 0.5in) aluminum plate.
K178, K700 and K254 mounted to a 406mm x 406mm x 12.5mm (16in x 16in x 0.5in) aluminum plate.
* See Engineering Reference page 297 for inertia discussion.

Pole Count:
K127 & K375 are 12
K700 & K500 are 8
K178 & K254 are 18

Servo Motors & Drives

Frameless Motors Series:

K032 to K0254 Motors

Dimensions

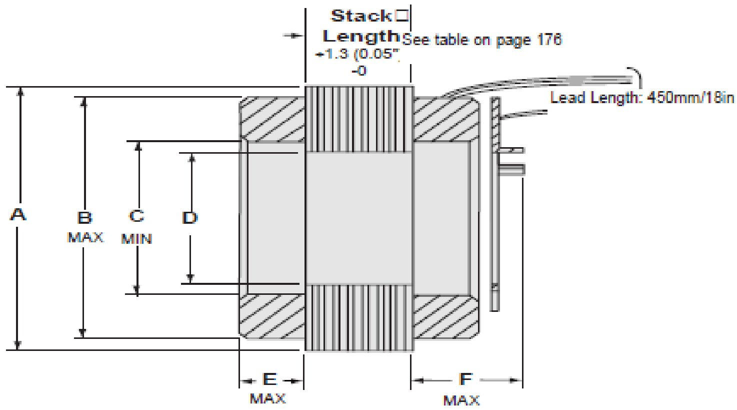

Stator Outline

Frame Size	A O.D. (mm)	A O.D. (in)	B End Turns O.D. (mm)	B End Turns O.D. (in)	C End Turns I.D. (mm)	C End Turns I.D. (in)	D I.D. (mm)	D I.D. (in)	E End Turns Length (mm)	E End Turns Length (in)	F Commutation Length (mm)	F Commutation Length (in)
K032	31.78 31.75	1.251 1.25	27.94	1.1	16.51	0.65	15.06 14.8	0.593 0.583	6.4	0.25	14.5	0.57
K044	44.48 44.42	1.751 1.749	40.64	1.6	26.16	1.03	22.35 22.09	0.88 0.87	7.9	0.31	16.5	0.65
K064	63.52 63.47	2.501 2.499	60.7	2.39	38.1	1.5	35.18 34.92	1.385 1.375	9.65	0.38	17.5	0.69
K089	88.92 88.87	3.501 3.499	85.8	3.38	54.6	2.15	53.47 53.21	2.105 2.095	9.91	0.39	17.5	0.69
K375	95.28 95.22	3.751 3.749	88.9	3.5	53.32	2.06	50.93 50.67	2.005 1.995	12.7	0.5	19.5	0.77
K127	127.02 126.97	5.001 4.999	122.17	4.81	74.17	2.92	72.49 72.23	2.854 2.844	12.7	0.5	19.5	0.77
K500	127.05 126.95	5.002 4.998	115.32	4.54	70.6	2.78	68.2 67.94	2.685 2.675	20.5	0.81	30.5	1.2
K178	177.88 177.72	7.003 6.997	172.72	6.8	111.51	4.39	110.64 110.38	4.355 4.345	20.3	0.8	*	
K700	177.88 177.72	7.003 6.997	158.24	6.23	117.6	4.63	115.19 114.93	4.535 4.525	18.8	0.74	*	
K254	254.07 253.92	10.003 9.997	253.26	9.971	165.1	6.5	157.61 157.35	6.205 6.195	19.6	0.77	*	

*integral commutation not available

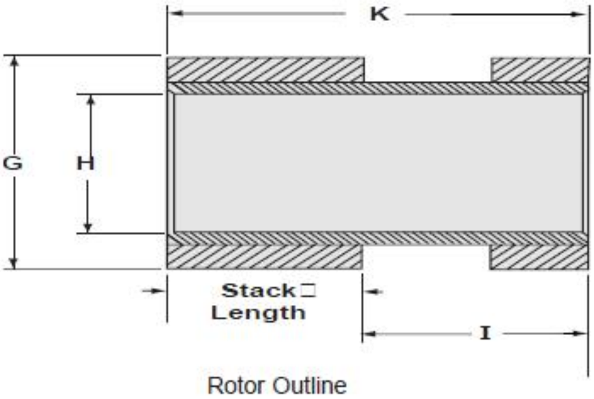

Rotor Outline

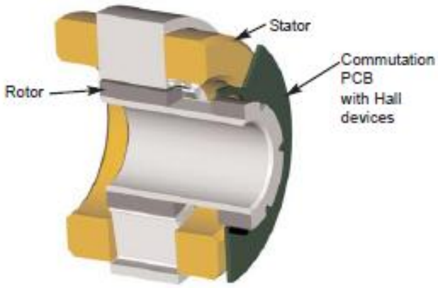

Figure 1.3
Kit Main Components

Frame Size	G Rotor O.D. (mm)	G Rotor O.D. (in)	H Rotor I.D. (mm)	H Rotor I.D. (in)	I Commutation Magnet Length (mm)	I Commutation Magnet Length (in)	K Rotor Length
K032	**13.94**	0.549	**7.62**	0.3	**13.21**	0.52	without Commutation:
	13.89	0.547	**7.59**	0.299			K = Stack Length + **0.76mm** (0.030in)
K044	**21.23**	0.836	**13.97**	0.55	**14.73**	0.58	
	21.18	0.834	**13.94**	0.549			with Commutation:
K064	**34.04**	1.34	**23.52**	0.926	**16.51**	0.65	K = Stack Length + **I** + **0.76mm** (0.030in)
	33.98	1.338	**23.49**	0.925			
K089	**51.84**	2.041	**40.64**	1.6	**16.71**	0.66	
	51.79	2.039	**40.61**	1.599			
K375	**49.28**	1.94	**38.1**	1.5	**19.56**	0.77	
	49.15	1.935	**38.07**	1.499			
K127	**71.15**	2.801	**58.42**	2.3	**19.56**	0.77	
	71.09	2.799	**58.39**	2.299			
K500	**66.54**	2.62	**50.83**	2.001	**28.52**	1.12	
	66.5	2.618	**50.8**	2			
K178	**109.2**	4.292	**95.76**	3.77	*		
	108.9	4.29	**95.73**	3.769			
K700	**113.54**	4.47	**95.25**	3.75	*		
	113.49	4.468	**95**	3.74			
K254	**156.16**	6.148	**140.46**	5.53	*		
	156.11	6.146	**140.44**	5.529			

*integral commutation not available

Servo Motors & Drives

Frameless Motors Series:
Winding Selection

The selection of a particular frame size and winding for an application is dependent on:

- Volume (diameter and length) requirement
- Power (torque and speed) requirement
- Voltage and current available or required

The first two items are dependent on the load and performance specifications of the application. They result in the selection of a particular frame size (032 through 254) and stack length.

The winding to be used will then be determined by voltage and current available or required.

Voltage: The bus voltage and maximum speed will determine the required voltage constant (K_E).

Current: The maximum load and acceleration will determine the amount of current required, determined by the torque constant (K_T) associated with the selected voltage constant.

Example: Assume a requirement of 1,000 RPM at 50 oz in

If a motor with a particular winding having K_E = 18.24 V/1,000 RPM and K_T = 24.62 oz in/amp is chosen, it will now require a voltage (BEMF) of 18 volts and current of 2 amp.

NOTE: K_E and K_T are directly proportional to each other. Increasing K_E will also increase K_T; Decreasing K_E will also decrease K_T.

The result is that as the voltage requirement changes, the current requirement changes inversely.

Bayside has a range of 27 windings available for each frame size and stack length, providing for virtually any practical combination of voltage and current required for your application.

The following pages show just a small representative sample of speed/torque curves for each of the 10 frame sizes available.

For the 044, 064, 089 and 127 frame sizes, the speed/torque curves are for stators that are used in the standard BM / GM motor products.

They make a good starting point for determining your specific application requirements and working with Bayside application engineers to choose the proper motor size and power.

The following table lists the range of K_E and K_T available for each of the 10 frame sizes.

Detailed information for all these windings can be found on the web site: www.baysidemotion.com

Frame Size	Stack Range (mm)	Stack Range (in)	K_E Range (V/1,000 RPM)	K_E Range (V/rad/sec)	K_T Range (Nm/amp)	K_T Range (oz in/amp)
K032	6.35 to 50.8	0.25 to 2.00	0.14 to 65.52	0.0013 to 0.625	0.0013 to 0.625	0.18 to 88.45
K044	6.35 to 50.8	0.25 to 2.00	0.28 to 126.3	0.0027 to 1.2	0.0027 to 1.2	0.38 to 170.6
K064	6.35 to 50.8	0.25 to 2.00	0.66 to 291.8	0.0063 to 2.78	0.0063 to 2.78	0.89 to 394
K089	6.35 to 50.8	0.25 to 2.00	1.35 to 605	0.013 to 5.77	0.013 to 5.77	1.83 to 817
K375	6.35 to 50.8	0.25 to 2.00	1.27 to 566	0.012 to 5.40	0.012 to 5.40	1.71 to 765
K127	12.7 to 50.8	0.50 to 2.00	3.73 to 827	0.036 to 7.88	0.036 to 7.88	5.04 to 1116
K500	12.7 to 50.8	0.50 to 2.00	3.38 to 714	0.032 to 6.81	0.032 to 6.81	4.56 to 964
K178	12.7 to 50.8	0.50 to 2.00	8.26 to 1716	0.079 to 16.4	0.079 to 16.4	11.18 to 2,323
K700	12.7 to 50.8	0.50 to 2.00	4.14 to 872	0.039 to 8.31	0.039 to 8.31	5.59 to 1,177
K254	12.7 to 50.8	0.50 to 2.00	11.44 to 2,537	0.109 to 24.2	0.109 to 24.2	15.5 to 3,425

NOTE: Longer stacks and special windings are available. Call **1-800-305-4555**

K032150-7Y

K_T = **0.051 Nm/amp** (7.19 oz-in/amp) R_{T-T} = 2.05 Ω I_{cont} = 3.6 amp
K_E = **0.051 v/rad/sec** (5.32 V/kRPM) L_{T-T} = 1.16 mH I_{peak} = 10.8 amp
E_{BUS} = 48 Vdc

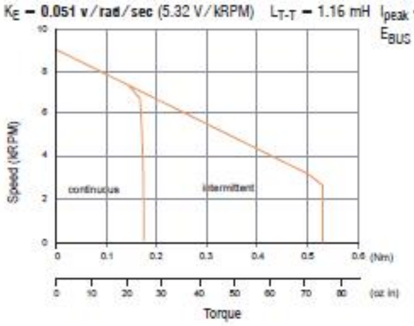

K044150-FY

K_T = **0.28 Nm/amp** (39.6 oz-in/amp) R_{T-T} = 11.8 Ω I_{cont} = 2 amp
K_E = **0.28 v/rad/sec** (29.3 V/kRPM) L_{T-T} = 12.5 mH I_{peak} = 6 amp
E_{BUS} = 160 Vdc

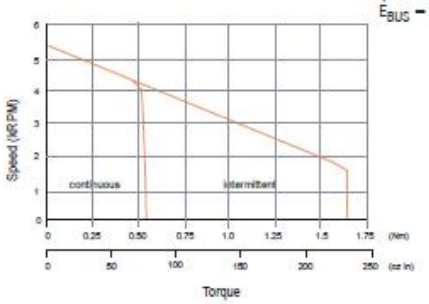

K044300-8Y

K_T = **0.28 Nm/amp** (39.6 oz-in/amp) R_{T-T} = 4.8 Ω I_{cont} = 3 amp
K_E = **0.28 v/rad/sec** (29.3 V/kRPM) L_{T-T} = 6.2 mH I_{peak} = 9 amp
E_{BUS} = 160 Vdc

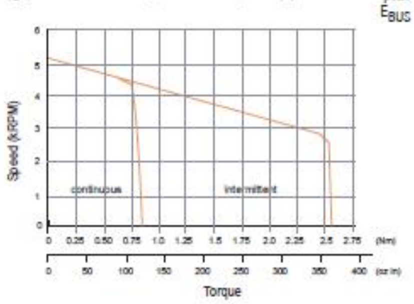

K064150-8Y

K_T = **0.33 Nm/amp** (46.1 oz-in/amp) R_{T-T} = 2.5 Ω I_{cont} = 6 amp
K_E = **0.33 v/rad/sec** (34.1 V/kRPM) L_{T-T} = 4.5 mH I_{peak} = 18 amp
E_{BUS} = 160 Vdc

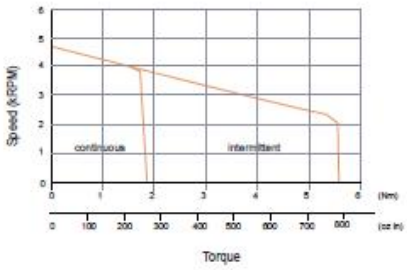

K064300-6Y

K_T = **0.42 Nm/amp** (59.9 oz-in/amp) R_{T-T} = 1.6 Ω I_{cont} = 7 amp
K_E = **0.42 v/rad/sec** (44.3 V/kRPM) L_{T-T} = 3.8 mH I_{peak} = 21 amp
E_{BUS} = 160 Vdc

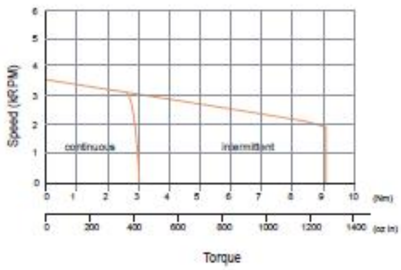

K375150-6Y

K_T = **0.41 Nm/amp** (57.92 oz-in/amp) R_{T-T} = 1.21 Ω I_{cont} = 10 amp
K_E = **0.41 v/rad/sec** (47.82 V/kRPM) L_{T-T} = 3.45 mH I_{peak} = 30 amp
E_{BUS} = 160 Vdc

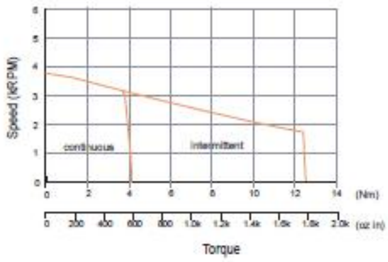

Frameless Motors Series:

Speed/Torque Curves

K089150-6Y

K_T = **0.43 Nm/amp** (61.6 oz-in/amp) $R_{T\text{-}T}$ = 1.2 Ω I_{cont} = 11 amp
K_E = **0.43 v/rad/sec** (45.6 V/kRPM) $L_{T\text{-}T}$ = 2.9 mH I_{peak} = 33 amp
E_{BUS} = 160 Vdc

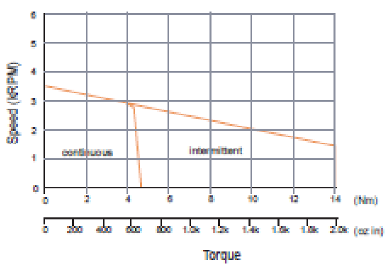

K089300-4Y

K_T = **0.54 Nm/amp** (75.8 oz-in/amp) $R_{T\text{-}T}$ = 0.73 Ω I_{cont} = 15 amp
K_E = **0.54 v/rad/sec** (56.1 V/kRPM) $L_{T\text{-}T}$ = 2.2 mH I_{peak} = 45 amp
E_{BUS} = 160 Vdc

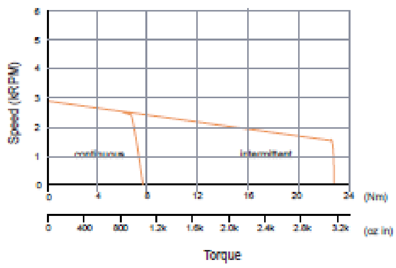

K127250-4Y

K_T = **0.61 Nm/amp** (86.9 oz-in/amp) $R_{T\text{-}T}$ = 0.35 Ω I_{cont} = 20 amp
K_E = **0.61 v/rad/sec** (64.2 V/kRPM) $L_{T\text{-}T}$ = 2.1 mH I_{peak} = 60 amp
E_{BUS} = 300 Vdc

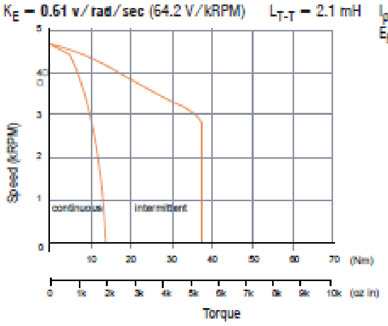

K127500-3Y

K_T = **0.92 Nm/amp** (130.4 oz-in/amp) $R_{T\text{-}T}$ = 0.34 Ω I_{cont} = 24 amp
K_E = **0.92 v/rad/sec** (96.4 V/kRPM) $L_{T\text{-}T}$ = 2.3 mH I_{peak} = 72 amp
E_{BUS} = 300 Vdc

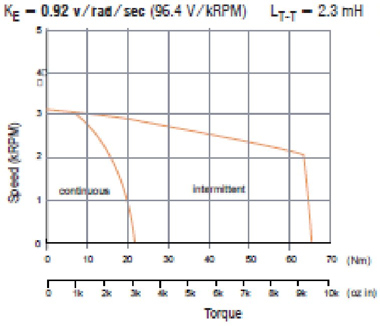

K500150-5Y

K_T = **0.45 Nm/amp** (63.78 oz-in/amp) $R_{T\text{-}T}$ = 0.49 Ω I_{cont} = 18 amp
K_E = **0.45 v/rad/sec** (47.19 V/kRPM) $L_{T\text{-}T}$ = 2.72 mH I_{peak} = 53 amp
E_{BUS} = 300 Vdc

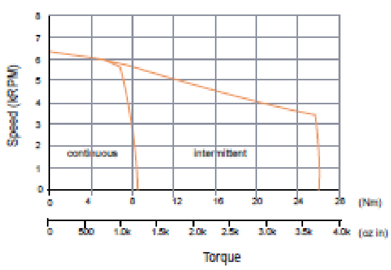

K178150-5Y

K_T = **0.93 Nm/amp** (130.5 oz-in/amp) $R_{T\text{-}T}$ = 0.37 Ω I_{cont} = 27 amp
K_E = **0.93 v/rad/sec** (96.2 V/kRPM) $L_{T\text{-}T}$ = 2.95 mH I_{peak} = 43 amp
E_{BUS} = 300 Vdc

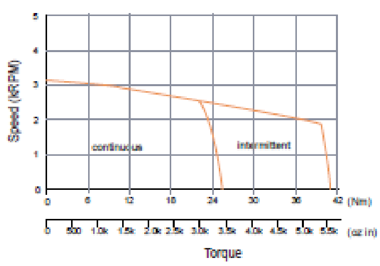

K700150-7Y

K_T = **0.78 Nm/amp** (110.35 oz-in/amp) R_{T-T} = 0.84 Ω I_{cont} = 18 amp
K_E = **0.78 v/rad/sec** (81.71 V/kRPM) L_{T-T} = 5.79 mH I_{peak} = 28 amp
E_{BUS} = 300 Vdc

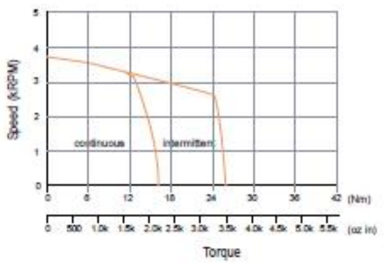

K254150-5Y

K_T = **1.42 Nm/amp** (199.7 oz-in/amp) R_{T-T} = 0.78 Ω I_{cont} = 34 amp
K_E = **1.42 v/rad/sec** (147.6 V/kRPM) L_{T-T} = 3.6 mH I_{peak} = 54 amp
E_{BUS} = 300 Vdc

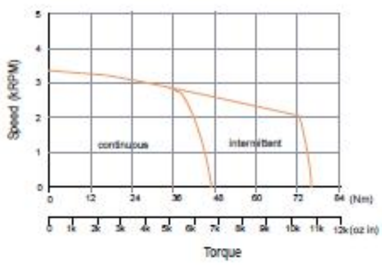

How to Order

Order Numbering Example: K 0 4 4 1 0 0 – E Y 3

MODEL	STACK LENGTH	WINDING(1)	CONNECTION	COMMUTATION
032	025 (0.25")	1	Y	1 = Without
044	050 (0.50")	2		2 = With Integral
064	075 (0.75")	3		3 = With External (2)
089	100 (1.00")	4		
375	150 (1.50")	5		
127	200 (2.00")	6		
500		7		
178		8		
700		9		
254		E		
		F		
		G		
		H		
		J		
		K		
		L		

(1) Consult Bayside (1-800-305-4555 or www.baysidemotion.com) for specific winding designations.
(2) For K178, K700 & K254 only

Bayside Kit Motors are supported by a worldwide network of offices and local distributors. Call 1-800-305-4555 for application engineering assistance or for the name of your local distributor. Information can also be obtained at www.baysidemotion.com.

Servo Motors & Drives

Specifications are subject to change without notice.

Appendix E: Data used in simulations

The following values are provided for by Prof. Dr. R. Babuska

Brushless DC Motor

Quantity	Symbol	Value
Rotor inductance	L	1.8E-3 H
Rotor resistance	R	6.81 Ohm
Torque constant	K	0.138 Nm/A
Rotor inertia	J	9.7E-5 Nm^2
Viscous damping	b	0.0012 Nms/rad

Piston

Quantity	Symbol	Value
Piston Area	Ap	2.4829 dm^2
Piston displacement per screw revolution (turn)	ps	0.025 dm

Air Compartment

Quantity	Symbol	Value
Air bulk modulus (elastance)	Ea	1E2 kPa
Air inertance	Ia	0.12 kg/m^4
Air flow resistance	Ra	800E-3

Lung Model

Quantity	Symbol	Value
Presumed stable lung resistance	RL	0.5 L/kPa
Presumed stable lung compliance	CL	1.1 kPa/L/s
Presumed unstable lung resistance	RL	0.5 L/kPa
Presumed unstable lung compliance	CL	0.5 kPa/L/s

The following values are provided by the datasheet from Maccon[10], an actuator manufacturing company. They're from the LAL series voice coils. Some values are changed, because demonstrating the concept of backdrivability being useful in lung simulators was more important than designing a real lung simulator.

Voice Coil

Quantity	Symbol	Value
Emf / velocity constant	Kf/Kg	100 N/A or Vs/m
Coil mass	M	1.6 kg
Coil resistance	R	4 Ohm
Coi inductance	L	2E-3 H
Friction coefficient	b	0
Piston area	Ap	2.4829 dm^2

The following values were chosen by the authors.

[10] http://www.maccon.de/en/actuators/voice-coil-actuators/lal.html

BLDC controller

Quantity	Symbol	Value
Controller gain	Gain	300
Alpha (corresponding to required phase lead)	Alpha	1/10
First break point	T	1/150

Voice coil controller

Quantity	Symbol	Value
Controller gain	Gain	1000 - 2500

Appendix F: MATLAB .m-files

To initialize SIMULINK simulations of the voice coil ‘parameters_voice_coil.m’ contains all the constants.

```
%====================================
% Mathematical Model of a Voice Coil
%====================================
% Reinier Doelman and Anton Delawari
%           15-5-2010
%====================================

clear all;

% ========== Parameters ===========
% Model: LAL500-050 from maccon.de (slightly modified)
% Electromagnetic force constant Kf
Kf = 100;      %[N/A]
% Elektromotive force / 'velocity' constant Kg
Kg = Kf;      %[Vs/m]=[N/A]
% Coil mass M
M = 1.6;       %[kg]
% Coil resistance R
R = 4;       %[Ohm]
% Coil inductance L1
L1 = 2E-3;      %[H]
% Friction coefficient
b = 0;
% Piston Area
Ap = pi*(2.54*7/20)^2; %[dm^2]

% Air Compartment
Ea = 1E2; %[kPa]
Ia = 0.12; %[kg/m^4]
Ra = 800E-3; %[kPa s/L]

% Lung Model
%   Instable lung parameters:   CL = 0.5; RL = 0.5;
%   Stable lung parameters:     CL = 0.5; RL = 1.1;
CL = 0.5; %[L/kPa]
RL = 1.1; %[kPa/L/s]

% ========== Controller function ===========
gain = 2500;
```

To initialize SIMULINK simulations of the BLDC 'Model_lung_parameters.m' contains all the constants.

```
%===================================
%      Parameters for the BLDC
%===================================
% Reinier Doelman and Anton Delawari
%           15-5-2010
%===================================

clear all;
close all;

% Piston
Ap = pi*(2.54*7/20)^2; %[dm^2]
ps = 10*0.0025; %[dm]

% Air Compartment
Ea = 1E2; %[kPa]
Ia = 0.12; %[kg/m^4]
Ra = 800E-3; %[kPa s/L]

% Lung Model
%   For more stable parameters choose
%   CL = 0.5, unstable 0.5
%   RL = 1.1, unstable 0.5
%   For unstable parameters choose
%   CL = 0.5
%   RL = 0.5
CL = 0.5; %[L/kPa]
RL = 1.1; %[kPa/L/s]

% Motor model
L = 1.8E-3; %[H]
R = 3*2.27; %[Ohm]
K = 0.138; %[Nm/A]
J = 9.7E-5; %[Nm2]
b = 0.0012; %[Nms/rad]

% Controller parameters
Kgain = 300;
alpha = 1/10;
T = 1/150;

% Transfer functions
%   Controller
Control = Kgain*tf([T 1],[alpha*T 1]);
%   BLDC
Motor = tf(K, [L*J (L*b+R*J) (R*b+K^2) 0]);
%   Actuator with controller
Actuator = Control*Motor/(1+Control*Motor);
%   Air Compartment
AirCompartment = tf([Ea Ea*Ra/Ia 0],[1 Ra/Ia Ea/Ia]);
%   Lung model
Lung = tf(CL/(Ap*ps),[RL*CL 1]);
%   Piston gain
Piston = Ap*ps;
%   Open loop system
System = Lung*Piston*AirCompartment*Actuator;
```

```
% Plots
%   Open loop system
figure(1)
margin(System);

%   Closed loop system
figure(2)
step(1/(1-System));

%   Controller open loop
figure(3)
margin(Control*Motor)

%   Step response on the actuator
figure(4)
time = 0:0.002:1;
step(Control*Motor/(1+Control*Motor), time)
```

To design a controller for the BLDC, the following file ‘motor_controller_design.m’ was used.

```
%===================================
%   Design for a BLDC controller
%===================================
% Reinier Doelman and Anton Delawari
%           15-5-2010
%===================================

% Motor controller design
close all;
clear all;

% ==== Parameters ====
%   Armature inductance
L = 1.8E-3;             %[H]
%   Armature resistance
R = 3*2.27;             %[Ohm]
%   Motor torque constant
K = 0.138;              %[Nm/A]
%   Total rotor-nut-bearing inertia
J = 9.7E-5;             %[Nm2]
%   Viscous friction coefficient (damping)
b = 0.0012;             %[Nms/rad]

% ==== Functions ====
% Motor transfer function
M = tf(K,[J*L (J*R+b*L) (b*R+K^2) 0]);

% Reduced order motor system: set L = 0
Mred = tf([K],[J*R (b*R+K^2) 0]);

% Controller function
Gain = 3;
s = tf('s');
Contrl = Gain;
```

```
% ==== Plots ====
figure(1)
bode(M)
title('Bode Plot of a Brushless DC Motor Model');

figure(2)
margin(Contrl*M);

figure(3);
T1 = (Contrl*M) /(1+Contrl*M);
T2 = (M) /(1+M);
time = 0:0.0001:0.4;
step(T1,'r', T2,'g--',time)
title('Step input on model+controller (red) en model (green, dashed)');

figure(4)
bode(Contrl*M / (1+ Contrl*M))
```

To design a controller for the voice coil, the following file ‘voice_coil_controller.m’ was used.

```
%====================================
% Mathematical Model of a Voice Coil
%====================================
% Reinier Doelman and Anton Delawari
%           15-5-2010
%        Controller Design
%====================================

clear all;
close all;

% ========== Parameters ===========
% Model: LAL500-050 from maccon.de (slightly modified)
% Electromagnetic force constant Kf
Kf = 100;     %[N/A]
% Elektromotive force / 'velocity' constant Kg
Kg = Kf;      %[Vs/m]=[N/A]
% Coil mass M
M = 1.6;      %[kg]
% Coil resistance R
R = 4;        %[Ohm]
% Coil inductance L1
L1 = 2E-3;     %[H]
% Friction coefficient
b = 0;
% Piston Area
Ap = pi*(2.54*7/20)^2; %[dm^2]
```

```
% ========== Coil Function ===========
Coil = tf(Kf,[(L1*M) (R*M+L1*b) (R*b+Kf*Kg) 0]);
Disturbance = Ap*tf([L1 R],[(L1*M) (R*M+L1*b) (R*b+Kf*Kg) 0]);

% ========== Controller function ===========
gain = 1200;
Control = gain;

% ========== Plots ===========
figure(1)
bode(Coil,'r', Coilred, 'g')
title('Bodeplot Voice Coil model and reduced model - no controller, open
loop');

figure(2)
margin(Coil*Control);
title('Bodeplot Voice Coil - with controller, open loop');

figure(3);
T1 = (Coil*Control)/(1+Coil*Control);
T2 = (Coil) /(1+Coil);
time = 0:0.01:4;
step(T1,'r',T2,'g',time)
title('Step input on Coil with (red) and without controller(green)');

figure(4)
T3 = (Disturbance)/(1+Disturbance*Control);
T4 = (Disturbance)/(1+Disturbance);
impulse(T3,'r', T4,'g')
title('Disturbance rejection with (red) and without controller(green),
closed loop');
```